THESIS FOR THE DEGREE OF DOCTOR OF PHILOSOPHY IN THERMO AND FLUID DYNAMICS

# Subcooled boiling flow in liquid-cooled internal combustion engines

SUDHARSAN VASUDEVAN

Department of Mechanics and Maritime Sciences

Division of Fluid Dynamics

CHALMERS UNIVERSITY OF TECHNOLOGY

Göteborg, Sweden 2022

Subcooled boiling flow in liquid-cooled internal combustion engines
SUDHARSAN VASUDEVAN
ISBN 978-91-7905-705-3



Doktorsavhandlingar vid Chalmers tekniska högskola
Ny serie nr. 5171
ISSN 0346-718X
Department of Mechanics and Maritime Sciences
Division of Fluid Dynamics
Chalmers University of Technology
SE-412 96 Göteborg
Sweden
Telephone: +46 (0)31-772 1000

Chalmers Reproservice
Göteborg, Sweden 2022

Subcooled boiling flow in liquid-cooled internal combustion engines
SUDHARSAN VASUDEVAN
Department of Mechanics and Maritime Sciences
Division of Fluid Dynamics
Chalmers University of Technology

# Abstract

Road transport sector contributes significantly to emission of carbon dioxide and other greenhouse gases, which negatively impact the global climate. Efficient management of energy, irrespective of the type of propulsion, has the potential to minimize fuel consumption and to reduce emission of greenhouse gases. This makes thermal (energy) management an indispensable part of automotive propulsion research and development. Cooling plays an important role in protecting the components from failure due to extreme thermal loads. An efficient cooling strategy, such as precision cooling, removes the excess heat precisely from the parts experiencing critical temperatures, without over cooling the component.

The thesis focuses primarily on numerical methodologies to explore the potential of local nucleate boiling for efficient cooling of internal combustion engines. Nucleate boiling is a heat transfer phenomenon involving a phase change process, where the liquid coolant vaporizes in the form of bubbles close to the heated surface. Occurrence of nucleate boiling, locally in the vicinity of hot spots, offers a significant potential for efficient precision cooling, but at the risk of encountering film boiling. Film boiling is encountered as a consequence of excessive boiling which leads to coalescence and agglomeration of vapor bubbles, resulting in formation of a thin vapor film, next to the heated surface. On account of the low thermal conductivity of the vapor, film boiling prevents cooling and could potentially lead to material failure. Therefore, tapping the potential of controlled local nucleate boiling is a preferable approach.

In the current work, a new semi-mechanistic wall boiling model is proposed that not only estimates the occurrence of boiling, but also the boiling heat flux and the extent of boiling. It is vital to know the extent of boiling in order to avoid, with sufficient margin, the risk of encountering film boiling. The proposed model is validated with results from channel flow experiments available in the literature. Further, the model is implemented in real engine simulations in both single phase and multiphase Computational Fluid Dynamics (CFD) frameworks. The model performance is evaluated by comparing the results of the simulations with relevant measurements. The model estimates the wall boiling heat flux with reasonably good accuracy and indicates the occurrence of excessive boiling with sufficient margin for industrial applications.

*To my family*

# Acknowledgements

To start with, I would like to thank my supervisor and mentor, Sassan Etemad, and my co-supervisor and examiner, Lars Davidson, for providing me this opportunity to pursue my doctoral studies. Sassan, thank you for all the insightful discussions and the exposure you have provided me during the course of this project. Lars, thank you for always finding time for our discussions and I really enjoy learning from you. Thank you both for constantly supporting me and you both are amazing!

A big thanks to all my industrial supervisors for sharing your perspective on the topic and your valuable inputs, which always led to interesting discussions. A special mention here to Mirko Bovo for always finding time for those interesting discussions regarding work, climbing and a lot more. I should admit that your energy and enthusiasm is highly contagious and I love working with you! Thank you Peter Båstedt for the wonderful data set from the engine rig and for all those interesting discussions around it, which provided this project a better perspective within the industry. I would also like to thank Stefan Eriksson and Mattias Ljungqvist for setting up the platform for the work done at Volvo Car Corporation and Aurobay. Thank you Babajimopoulos Aristotelis and Oscar Bergman for supporting me with the CHT model and for all the interesting discussions. Thank you Magnus Brogeby, Anders Wedin and Jonathan Hafstöm for your support and valuable inputs to work with the CHT model of the truck engine at AB Volvo. We all really missed Kaj Johansson and his enthusiasm towards the realization of this project. In the lab at Chalmers: Isak Jonsson, a huge thanks for all your help and support in designing and setting up the rig. Also, a big thanks to Patxi Daniel Acero and Edward Hadziavdic for putting up with all the leaks and constantly helping me with encouragement, ideas and hands to fix them. Thank you Zahra Tari for your support in the initial stages of designing the rig.

A big thanks to Ananda, Niklas, Magnus, Debarshee, Gonzalo, Guglielmo, Vinicius, Marily and all other wonderful people in the division of Fluid Dynamics for all the good times we had! Thank you Srdjan Sasic for always having me under your surveillance, Haha! Also, a special thanks to all those who helped me practice Swedish in the department, especially Blagica and Ulla who put up a lot with my crazy pronunciations and vocabulary!

To my family: Amma, Appa (Sudhavalli, Vasudevan) and Madhavan, all this wouldn't have been possible without your constant encouragement and support. Sindhuja, your patience, understanding and belief in me has often reinforced my own confidence and helped me stay more positive and focused. You all are super awesome and I am forever grateful! Of course, my personal circle is incomplete without all my wonderful friends and family who've always been by my side. Thank you all!

This acknowledgement would be incomplete without thanking the Swedish society and the educational system for providing such a fantastic opportunity and environment for me to learn and grow. To this end, I would like to acknowledge and thank Chalmers University of Technology for supporting and the Swedish Energy Agency, Volvo Car Corporation and AB Volvo for financing my graduate education.

Sudharsan Vasudevan

Göteborg, September 2022

# ABBREVIATIONS

| | | |
|---|---|---|
| BDL | – | Boiling Departure Lift-off |
| BBM | – | Blended Boiling Model |
| CFD | – | Computational Fluid Dynamics |
| CHT | – | Conjugate Heat Transfer |
| FDB | – | Fully Developed boiling |
| ICE | – | Internal Combustion Engine |
| ONB | – | Onset of Nucleate Boiling |
| RPI | – | Rensselaer Polytechnic Institute (boiling model) |

# NOMENCLATURE

**Greek letters**

| | | |
|---|---|---|
| $\phi$ | Contact angle | rad |
| $\Pi$ | Probability of bubble interaction | |
| $\sigma$ | Surface tension | $\mathrm{N\,m^{-1}}$ |

**Roman letters**

| | | |
|---|---|---|
| $\Delta T_{sat}$ | Wall superheat | K |
| $F$ | Forced convection enhancement factor | |
| $h_{fc}$ | Single phase forced convection heat transfer coefficient | $\mathrm{W\,m^{-2}\,K^{-1}}$ |
| $h_{lv}$ | Latent heat of vaporization | $\mathrm{J\,kg^{-1}}$ |
| $M$ | Molecular mass | $\mathrm{kg\,mol^{-1}}$ |
| $p_\infty$ | Vapor pressure in a planar liquid-vapor interface | $\mathrm{N\,m^{-2}}$ |
| $p_l$ | Liquid pressure | $\mathrm{N\,m^{-2}}$ |
| $p_v$ | Pressure inside vapor bubble | $\mathrm{N\,m^{-2}}$ |
| $q_{BBM}$ | Heat flux from Blended Boiling Model | $\mathrm{W\,m^{-2}}$ |
| $q_{BDL}$ | Heat flux from Boiling Departure Lift-off model | $\mathrm{W\,m^{-2}}$ |
| $q_e$ | Evaporation heat flux | $\mathrm{W\,m^{-2}}$ |
| $q_{fc}$ | Single phase forced convection heat flux | $\mathrm{W\,m^{-2}}$ |
| $q_{nb}$ | Nucleate boiling heat flux | $\mathrm{W\,m^{-2}}$ |
| $q_q$ | Quenching heat flux | $\mathrm{W\,m^{-2}}$ |
| $q_{Roh}$ | Heat flux from Rohsenow's correlation | $\mathrm{W\,m^{-2}}$ |
| $q_{wall}$ | Wall heat flux | $\mathrm{W\,m^{-2}}$ |
| $R$ | Universal gas constant | $\mathrm{J\,K^{-1}\,mol^{-1}}$ |
| $r$ | Vapor bubble radius | m |
| $R_a$ | Average surface roughness height | m |
| $r_c$ | cavity mouth radius | m |
| $S$ | Nucleate boiling suppression factor | |
| $T_l$ | Liquid temperature | K |
| $T_{sat}$ | Liquid saturation temperature | K |
| $T_{wall}$ | Wall temperature | K |
| $v_l$ | Specific volume of liquid | $\mathrm{m^3\,kg^{-1}}$ |
| $v_v$ | Specific volume of vapor | $\mathrm{m^3\,kg^{-1}}$ |
| $z$ | Bubble height | m |

# List of publications

**This thesis is based on the following appended papers:**

**Paper A** S. Vasudevan, S. Etemad, L. Davidson, and G. M. Villar. Numerical model to estimate subcooled flow boiling heat flux and to indicate vapor bubble interaction. *International Journal of Heat and Mass Transfer* **170** (2021), 121038

**Paper B** P. Båstedt, S. Vasudevan, and M. Bovo. Subcooled Flow Boiling in High Power Density Internal Combustion Engines I: Thermal Survey Measurement Campaign. *SAE Int. J. Engines* **16**.1 (2023). `https://doi.org/10.4271/03-16-01-0002.`

**Paper C** S. Vasudevan and M. Bovo. Subcooled Flow Boiling in High Power Density Internal Combustion Engines II: Numerical Modeling. *SAE Int. J. Engines* **16**.1 (2023). `https://doi.org/10.4271/03-16-01-0003.`

**Paper D** S. Vasudevan, S. Etemad, L. Davidson, and M. Bovo. Comparative analysis of single and multiphase numerical frameworks for subcooled boiling flow in an internal combustion engine coolant jacket. *Applied Thermal Engineering* (revised manuscript submitted)

**Paper E** S. Vasudevan and I. Jonsson. *Design and construction of a rig for investigation of subcooled boiling flow.* Tech. rep. Chalmers University of Technology, 2022

# Division of work

The author, S. Vasudevan, developed the proposed boiling model, presented in Paper A, with guidance provided by Assoc. Prof. S. Etemad and Prof. L. Davidson. The engine rig tests, presented in Paper B, was planned and executed by P. Båstedt. The test results were post-processed by S. Vasudevan. The interpretation of the results and the calculations related to measurement uncertainties were done by S. Vasudevan with the guidance of Dr. M. Bovo and P. Båstedt. The new boiling model was implemented using the user code functionality in Star-CCM+ by S. Vasudevan in both the single phase and the mixture multiphase simulation frameworks. S. Vasudevan also performed all numerical simulations, presented in both Paper C and Paper D. Assoc. Prof. S. Etemad and Prof. L. Davidson provided guidance and helpful discussions for the simulations on the channel flow geometry in Paper D. The guidance and support for the engine simulations in both Paper C and Paper D was provided by Dr. M. Bovo, who also provided the CFD-CHT simulation model of the engine. The design of the boiling rig and the relevant calculations, presented in Paper E, was done by S. Vasudevan with guidance and support from Dr. I. Jonsson.

# Contents

# Part I

# Extended Summary

# 1

# Introduction

Emission of greenhouse gases has a direct effect on the global climate. Emissions from various greenhouse gases are measured in terms of Carbon dioxide ($CO_2$) equivalent. The amounts of other gases are converted to equivalent amount of carbon dioxide based on their respective global warming potential, in order to estimate the $CO_2$ equivalent. Transport sector is one of the major contributors to emission of greenhouse gases. In Sweden, domestic transportation contributes to roughly 30% of total $CO_2$ equivalent emissions [6]. Of this, the contribution from the road transport sector is the highest, accounting for 14134 kt $CO_2$-eqv. of the 15032 kt $CO_2$-eqv. in year 2020. The unit kt $CO_2$-eqv. stands for kilo tonnes of carbon dioxide equivalent. Figure 1.1 shows the emission data of green-house gases from road vehicles in Sweden. Although there has been

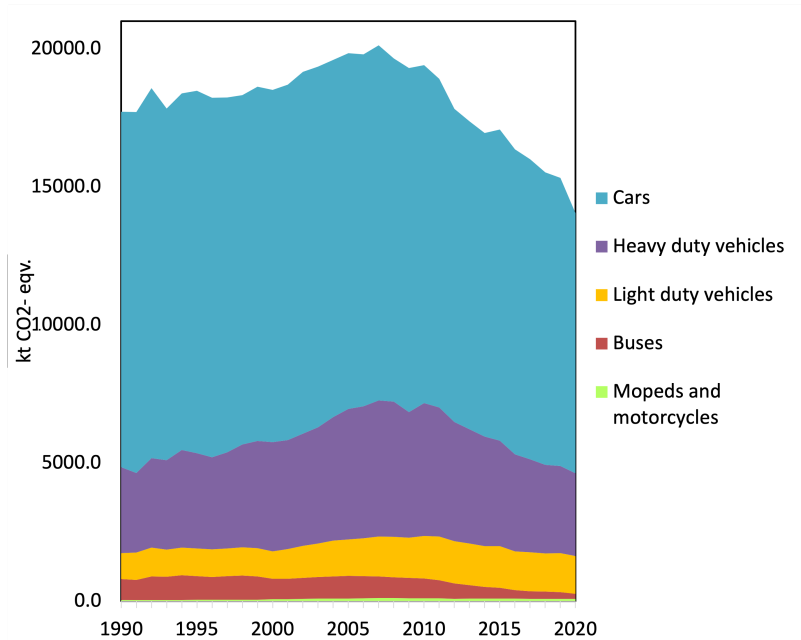


Figure 1.1: *Emission of greenhouse gases from road vehicles in kt $CO_2$-eq, considering only domestic transport in Sweden, statistikmyndigheten SCB (1990-2020) [6].*

consistent efforts in mitigating these emissions since 1990, the effect of emissions on the climate is still a topic of serious concern. This is also evident from Figure 1.1, where the measures for minimizing emissions are evident since 2012. Further, the advent of alternate propulsion methods in road vehicles (battery electric vehicles, vehicles operating with alternate fuels, fuel-cell powered vehicles, etc.) is a promising step towards minimizing emission of greenhouse gases.

Regardless of the source of energy for propulsion, cooling is an indispensable part of the automotive and marine propulsion in order to protect components experiencing critical temperatures. However, over-cooling the components, i.e., cooling of parts that do not exceed the critical temperature, leads to waste of energy.

Narrowing down the scope of this discussion to Internal Combustion Engines (ICEs), a recent trend in increasing specific power, the ratio of power to stroke volume, is realized. This trend is predominantly a result of consistent effort to downsize engines for (a) improving fuel efficiency (b) accommodating an electric propulsion, i.e., hybridization and (c) increasing the load carrying capacity (in case of heavy duty vehicles). Hence, engines have become smaller and for many car engines, the number of cylinders have been reduced, resulting in increased power density. Consequently, the engine structure experiences higher thermal loads, i.e., the engine components experience high temperatures. This excess heat is to be removed efficiently in order to preserve the structural integrity of the engine.

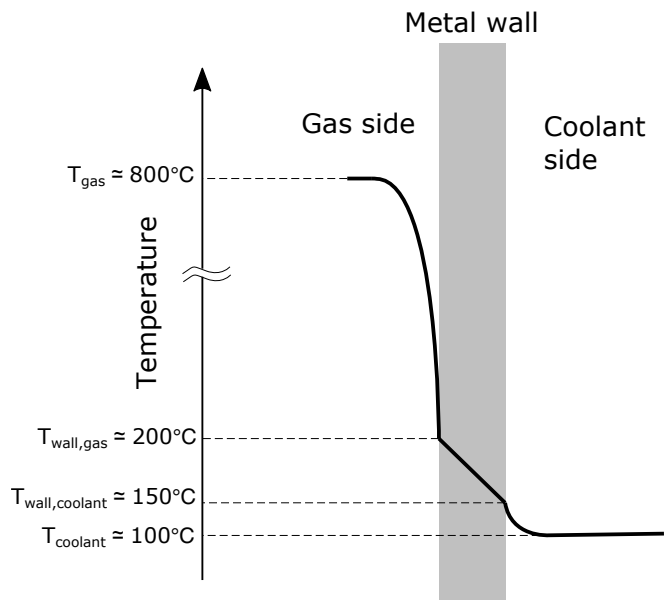


Figure 1.2: *Schematic representation of heat transfer from the combustion/gas side to the coolant side in an engine cylinder head.*

A schematic representation of heat transfer from the combustion chamber to the coolant is shown in Figure 1.2. The values of temperature specified are indicative of a four-cylinder passenger car petrol engine, operating at the maximum power load. Three major resistances to heat transfer are evident from Figure 1.2: resistance to convective heat transfer on the combustion/gas side, resistance to heat transfer by conduction in the cylinder wall and the resistance to convective heat transfer on the coolant side. In case of a cylinder block with a different material for the liner, the temperature distribution accounts for the resistance to heat conduction in both the materials. However, the thermal resistance on the gas side is significantly higher compared to the other resistances [7]. Therefore, any small change to the coolant side heat transfer does not alter the in-cylinder combustion process significantly. However, the coolant side heat transfer determines the operating temperature of the engine structural components and is therefore a crucial factor to be considered in engine design.

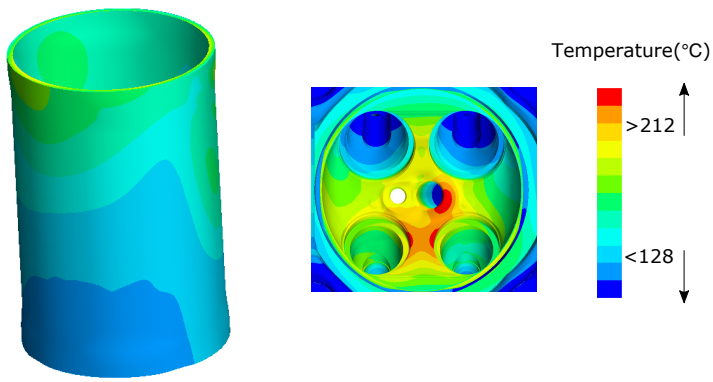


Figure 1.3: *Temperature distribution on the (a) cylinder liner and (b) flame deck of a four-cylinder passenger car petrol engine (blue-low, red-high).*

A conventional cooling system with a large cooling fan and pump is a parasitic load on the engine power output. The cooling packages and the cooling fans have already reached a size that challenges the spacial constraints in vehicles. Further, speeding up the coolant pump often leads to problems associated with cavitation. Moreover, since the fan power consumption is proportional to the cube of its operating speed, the fan consumes a significant portion of the additional power output from the engine.

The thermal load experienced by the engine structure is spatially non-uniform. Figure 1.3 shows local hot spots, resulting from an uneven distribution of thermal load on the liner and flame deck of a four-cylinder passenger car petrol engine. Uniform forced convection cooling might excessively cool the regions which do not need much cooling. This leads to unintentional loss of thermal energy. It might yet be insufficient for cooling the hot spots experiencing critical temperatures. Inevitably, an efficient cooling strategy is an absolute necessity. Precision cooling is considered as an effective strategy to minimize unintended

heat loss. Precision cooling means removal of excess heat from thermally critical regions in a component without excessively cooling the other non-critical regions.

Precision cooling has been studied using prototype engines to understand its influence on engine weight, temperature distribution in the engine components, the thermodynamic cycle, engine warm up conditions, emissions etc [8–12]. Robinson et al. [13] who reviewed a number of precision cooling studies, presented benefits of precision cooling. These benefits include lower friction as a result of higher operating temperature, faster engine warm-up, improved knock resistance, lower cylinder-to-cylinder variability, lower weight and improved vehicle cabin heating. All these contribute to efficient engine operation, leading to lower fuel consumption and emissions. The benefits also portray that precision cooling has an overall positive impact on the complete vehicle thermal management. The focus of this thesis is on exploring the potential of nucleate boiling as a technique for enhanced precision cooling of internal combustion engines.

# 2 Aim

Critical components in the engine structure often experience high temperatures. Nucleate boiling is encountered when the local surface temperature of the engine component in the coolant-solid interface is higher than the coolant saturation temperature. Such high temperature causes vaporization of coolant in the form of discrete vapor bubbles on the heated surface, which grow in size, eventually detach from the surface and condense into the liquid bulk. Thus, nucleate boiling is a phenomenon characterized by vapor bubbles created as a result of phase change in a liquid-cooled system and their interactions with the liquid coolant and the heated surface. On account of the phase change process, occurrence of nucleate boiling results in an exponential increase in heat transfer rate compared to forced convection heat transfer.

As explained in more detail in the subsequent chapters, the advantages of local nucleate boiling as a viable option for precision cooling comes with an upper limit. Excessive boiling leads to coalescence and agglomeration of vapor bubbles on the heated surface, eventually resulting in the formation of a vapor film which is known as film boiling. The low thermal conductivity of vapor reduces heat transfer significantly and prevents cooling. As a result, the component experiences a sudden and rapid increase in temperature which could potentially be detrimental to its structural integrity. Therefore, controlled local nucleate boiling is the key to an efficient precision cooling strategy.

With this background, the primary aims of the current work are formulated as follows.

- Study existing experimental and numerical works on nucleate boiling, relevant to heat transfer in coolant jacket of internal combustion engines, in order to
  - understand the complex mechanical and thermal interactions between the phases involved,
  - gain insight into various physical mechanisms involved in nucleate boiling and
  - understand quantitatively the factors influencing the heat transfer in nucleate boiling.
- Suggest improvements to existing numerical wall boiling models and develop a new model, that can be implemented in CFD in order to

  - estimate accurately the wall boiling heat flux in the boiling regime useful to precision cooling and
  - predict the extent of boiling so as to obtain an upper limit to avoid film boiling.
- Understand the heat transfer in the coolant jacket of internal combustion engines, from engine rig test data, in line with the theory of nucleate boiling.
- Evaluate the performance of the proposed wall boiling model in the coolant jacket of an automotive engine, based on engine rig test data, and present the advantages and limitations of the numerical methodology.

# 3

# Subcooled boiling flow

Nucleate boiling is classified into pool boiling or flow boiling, based on the nature of the flow in the liquid bulk. Boiling occurring on a heated surface submerged in a stagnant liquid bulk is known as pool boiling, whereas, the one occurring on a heated surface in a forced flow of liquid is known as flow boiling. More heat is transferred in flow boiling compared with pool boiling, since the additional heat transfer due to forced convection is significantly higher than its natural convection counterpart in pool boiling.

Nucleate boiling is classified based on the temperature of the liquid bulk. The boiling is said to be saturated if the temperature of the liquid bulk equals its saturation temperature and subcooled if the bulk liquid temperature is lower than its saturation temperature. The vapor bubbles nucleating on the heated surface condense into the liquid bulk in case of subcooled boiling, whereas no condensation occurs in saturated boiling. As a consequence, the vapor concentration is limited to the superheated liquid close to the heated wall in subcooled boiling. However, vapor is also present in the liquid bulk in the case of saturated boiling. Most internal combustion engines are cooled by forced flow of liquid coolant with the inlet bulk temperature below its saturation temperature. Even when the engine operates at maximum power, the temperature of the coolant at the engine outlet is still below its saturation temperature. Hence, the discussions in the rest of the thesis are restricted to the phenomenon of subcooled boiling flow.

## 3.1 Physical mechanisms influencing heat transfer

Subcooled boiling flow is a complicated phenomenon, characterized by various physical mechanisms. These mechanisms are characterized by the interactions between the heated solid, the liquid coolant and the coolant vapor bubbles. They account for both mechanical and thermal interactions between the phases and thereby, influence the heat transfer. Shoji [14] and Steiner et al. [15] have explained these thermal and mechanical interactions which influence the heat transfer in subcooled boiling flow. The interactions between the heated solid, the liquid coolant and the coolant vapor bubbles are depicted in Figure 3.1. The phenomenon of subcooled boiling flow includes

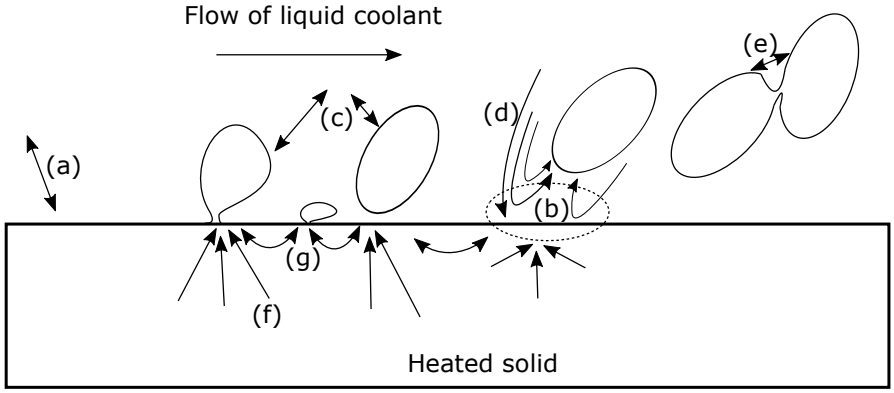


(a) Single phase forced convection heat transfer
(b) Surface quenching
(c) Interaction between coolant vapor bubbes and liquid coolant
(d) Micro-convection
(e) Interaction between coolant vapor bubbles
(f) Heat transfer by conduction within the solid
(g) Interaction between nucleation sites

Figure 3.1: *Interaction between phases in subcooled boiling flow.*

- Interaction between heated solid and liquid coolant:
  - The interaction between the liquid bulk and the area of the heated surface not covered by the vapor bubbles contribute to the single phase forced convection heat transfer.
  - The void created by a vapor bubble detached from its nucleation site is filled in by an inrush of subcooled liquid from the bulk. This inrush of subcooled liquid cools down the vicinity of the nucleation site below the temperature required for vapor bubble nucleation. This is termed as 'surface quenching'[15].
- Interaction between liquid coolant and vapor bubbles:
  - The inertial forces of the liquid bulk flow influence bubble growth, bubble detachment and trajectory of a detached vapor bubble.
  - The hydrodynamic forces resulting from a growing vapor bubble influence liquid velocity locally.
  - Liquid entrainment in the wake of a detached vapor bubble contributes to mixing of the subcooled liquid from the bulk with the superheated liquid layer close to the wall. This enhances the convective heat transfer locally and is termed as 'microconvection'[15].
  - When the boiling intensity is large, the heated surface is covered by a large number of vapor bubbles, which potentially influences the flow field close to the heated wall.

  - The thermal interaction between the liquid and the vapor bubbles includes the latent heat transfer during evaporation and condensation. Evaporation occurs in the macro- and micro-layer close to the foot of the bubble. Condensation occurs at the vapor-liquid interface at the bubble tip, when the bubble size is larger than the thickness of the near-wall superheated layer. Latent heat transfer also occurs when a detached vapor bubble condenses into a subcooled surrounding.

- Other interactions:
  - Interaction between vapor bubbles that could potentially form larger vapor bubbles or vapor column or even clouds of vapor.
  - The energy required for vapor bubble growth at the nucleation site is extracted from the solid surface, thereby bringing down the surface temperature locally around the nucleation site. The resulting spatial non-uniformity in surface temperature results in heat transfer by conduction within the heated solid. Similarly, the liquid in the vicinity of a nucleation site, experiencing surface quenching, needs to be heated again, to attain superheated conditions required for the nucleation of another vapor bubble. The energy required for this recovery is also extracted from the heated solid and this in turn contributes to conductive heat transfer within the solid.
  - The temperature of the heated surface is spatially non-uniform on account of presence of multiple nucleation sites. This results in exchange of thermal energy between the nucleation sites by heat conduction.
  - Interaction between nucleation sites also includes activation of a dormant nucleation site due to vapor residue from a neighbouring active site and deactivation of an active nucleation site due to flooding following bubble detachment from a neighbouring site [16].

While it is important to understand the underlying physical mechanisms in the boiling phenomenon, the key challenges to boiling research are to estimate their quantitative effects [15] and to understand the interaction between these physical mechanisms [14].

## 3.2 Boiling curve and boiling regimes

The heat transfer in subcooled boiling flow depends on several physical mechanisms, characterized by mechanical and thermal interaction between the heated solid, the liquid coolant and the coolant vapor bubbles. The dominance of one or more of these physical mechanisms depends on the prevailing thermal and flow conditions. Based on the dominant physical mechanisms under given conditions, various boiling regimes are identified. The boiling regimes associated with subcooled boiling flow are depicted on a boiling curve. The boiling curve is a plot of wall heat flux vs. wall surface temperature.

A boiling curve qualitatively depicting various boiling regimes in subcooled boiling flow is shown in Figure 3.2.

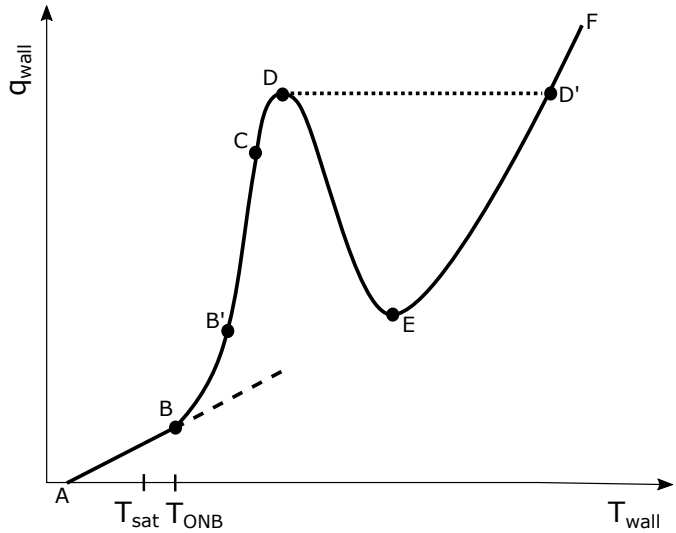


Figure 3.2: *Qualitative boiling curve indicating regimes in subcooled boiling flow. B- Onset of boiling; D- Critical heat flux; E- Leidenfrost point; AB- Single phase forced convection; BC- Partial boiling; BB'- Isolated bubbles; CD- Fully developed boiling; DE- transition boiling (encountered in a wall surface temperature controlled system); EF- Film boiling. In a wall heat flux controlled system, wall temperature increases along DD′ eventually resulting in film boiling. Occurrence of nucleate boiling (B-D) results in exponential increase in wall heat flux for a small increase in wall temperature.*

Consider the flow of liquid coolant in a channel, heated from its bottom surface. The heating is achieved either by controlling the wall heat flux or the wall surface temperature. Let us consider a wall surface temperature controlled system, where the temperature of the surface in contact with the liquid coolant is controlled. Initially, when the wall surface temperature is lower than the liquid saturation temperature, $T_{sat}$, of the coolant, sensible heat is transferred from the wall to the coolant by convection. This is known as the single phase forced convection regime, occurring in the interval A-B in Figure 3.2.

Increasing the wall surface temperature a few degrees above the saturation temperature causes vapor bubbles to nucleate on the surface of the heater and this is known as Onset of Nucleate Boiling (ONB), denoted as B in Figure 3.2. The temperature at onset of nucleate boiling, denoted by $T_{ONB}$, depends on the system pressure, the local velocity and the local temperature of the coolant. The local velocity and the local temperature of the coolant, in turn, depend on the bulk velocity and the bulk temperature. The onset of nucleate boiling also depends on other microscopic properties, such as micro-structure of the heated surface in contact with the coolant, deposits and contaminants on the surface, amount of dissolved gas in the coolant, etc.

With increasing surface temperature, after the onset of nucleate boiling, the population of vapor bubbles nucleating on the heated surface increases steadily, thereby increasing the heat transfer rate. This regime is known as the partial boiling regime, occurring in the interval B-C in Figure 3.2. Occurrence of nucleate boiling entails several additional mechanisms of the heat transfer compared with the heat transfer by single phase forced convection only. Latent heat transfer during bubble growth, additional turbulence due to bubble nucleation, detachment and collapse and surface quenching after bubble detachment are some key mechanisms that contribute to an exponential increase in heat transfer rate. In the partial boiling regime, the vapor bubbles are initially well separated spatially and are isolated from each other. This is identified as the isolated bubbles regime, as a sub-regime within the partial boiling regime, occurring in the interval B-B′ in Figure 3.2. With increasing vapor bubble population, as a result of increase in wall surface temperature, the vapor bubbles nucleate in close proximity and thereby start interacting with each other. With increase in bubble population and bubble interactions, the area on the heated surface in contact with liquid coolant is reduced, thereby decreasing the effect of heat transfer by forced convection.

With further increase in wall surface temperature, the vapor bubble population and interactions increase to such an extent that the heated surface is completely covered with nucleating and collapsing vapor bubbles. Under such conditions, the effect of forced convection on heat transfer is negligible and this regime is known as Fully Developed Boiling (FDB), occurring in the interval C-D in Figure 3.2. In the FDB regime, the mechanism of heat transfer is similar to that in pool boiling. Any further increase in wall temperature causes the vapor bubbles to coalesce and form clouds of vapor which in turn, owing to low thermal conductivity of vapor, impedes heat transfer from the surface of the heated solid. The maximum heat flux attained after FDB before the deterioration starts is known as critical heat flux, denoted as D in Figure 3.2.

Once the critical heat flux is attained, in a system in which the wall heat flux is controlled, any increase in input heat flux results in a rapid increase in wall surface temperature eventually leading to film boiling, along the dotted line D-D′ in Figure 3.2. However, if the wall surface temperature is controlled, any further increase in temperature results in a decrease in wall heat flux, in what is known as the transition boiling regime. The conditions in the internal combustion engine are more similar to a wall surface temperature controlled system rather than a wall heat flux controlled system, where the engine wall temperatures are determined by the temperature of the hot gases resulting from the combustion process. The transition boiling regime, occurring in the interval D-E in Figure 3.2, is characterized by agglomeration of vapor bubbles on the surface of the heated surface to form vapor clouds and the periodic detachment of these clouds of vapor from the heated surface. Any further increase in wall temperature leads to the formation of a thin vapor film over the heated surface and the heat is transferred by single (vapor) phase convection and radiation. This is known as the film boiling regime, occurring in the interval E-F in Figure 3.2. The maximum wall surface temperature attained is limited by the melting point of the metal. Encountering transition and film boiling regimes could be detrimental to the structural integrity of the component being cooled.

## 3.3 Vapor bubble formation and growth

The theory of formation and growth of a vapor bubble in a superheated liquid surrounding is the starting point and the basis for understanding the phenomenon of boiling and its numerical modelling. The theory explained by Collier and Thome [17] in this regard is presented here. The mechanical equilibrium of a vapor bubble nucleus of radius $r$ in a liquid at a superheated temperature $T_l$ and pressure $p_l$ reads

$$p_v - p_l = \frac{2\sigma}{r} \tag{3.1}$$

where, $p_v$ is the vapor pressure inside the nucleus and $\sigma$ is the surface tension at the liquid-vapor interface. Due to the curvature of the interface, this vapor pressure is fractionally lower than the vapor pressure, $p_\infty$, in a planar liquid-vapor interface. Rewriting the above equation in terms of the vapor pressure of a planar liquid-vapor interface results in

$$p_\infty - p_l = \frac{2\sigma}{r}\left(1 + \frac{v_l}{v_v}\right) \tag{3.2}$$

where, $v_l$ and $v_v$ are the specific volume of the liquid and the vapor, respectively. This pressure difference is recast into a temperature difference using the Clausius-Clapeyron equation. The Clausius-Clapeyron equation reads,

$$\frac{dp}{dT} = \frac{h_{lv}}{T(v_v - v_l)} \tag{3.3}$$

Assuming the vapor to be an ideal gas and that it obeys the ideal gas law, i.e.,

$$pv_v = \frac{RT}{M} \tag{3.4}$$

and further if the liquid specific volume is small relative to that of the vapor ($v_l << v_v$), Equation 3.3 is rewritten as

$$\frac{1}{p}dp = \frac{h_{lv}M}{RT^2}dT \tag{3.5}$$

Integrating the above equation from $p_l$ to $p_\infty$ on the left hand side and from $T_{sat}$ to $T_l$ on the right hand side,

$$ln\left(\frac{p_\infty}{p_l}\right) = \frac{h_{lv}M}{RT_lT_{sat}}(T_l - T_{sat}) \tag{3.6}$$

Substituting for $p_l/p_\infty$ from Equation 3.2 in the Equation 3.6 gives

$$T_l - T_{sat} = \frac{RT_{sat}T_l}{h_{lv}M} ln\left[1 + \frac{2\sigma}{p_l r}\left(1 + \frac{v_l}{v_v}\right)\right] \tag{3.7}$$

Collier and Thome further state that if $v_v \gg v_l$ and $\frac{2\sigma}{p_l r} \ll 1$, the above equation simplifies to

$$T_l - T_{sat} = \frac{2\sigma RT_{sat}^2}{p_l h_{lv} M r} \tag{3.8}$$

Equation 3.8 gives the criterion for minimum liquid superheat required for a stable vapor bubble nucleus of radius $r$ to exist. It is to be noted that with a higher liquid super heat existence of a smaller vapor bubble nucleus is possible. However, given that a stable vapor bubble nucleus exists, a higher superheat will result in growth of the vapor bubble.

### 3.3.1 Criterion for onset of nucleate boiling

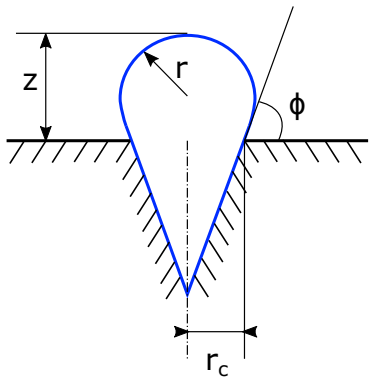


Figure 3.3: *Spherical vapor bubble nucleating from a conical cavity.*

Hsu[18] postulated that, the nucleation of a stable vapor bubble occurs when the liquid temperature at the tip of the vapor bubble exceeds the minimum temperature required for the existence of a stable vapor nucleus given by Equation 3.8. With this postulate and considering highly idealized conditions, he derived an analytical expression for the criterion for onset of nucleate boiling. Hsu considered the nucleation of a spherical vapor bubble from a conical cavity in a quiescent liquid. Hsu assumed that the cavity mouth has a circular cross section and the temperature of the quiescent liquid decreases linearly from the wall. The nucleation of a spherical vapor bubble of radius $r$ nucleating from a conical cavity with a cavity mouth radius $r_c$ is shown in Figure 3.3. The bubble height, i.e., the distance of the bubble tip from the wall, is denoted by $z$ and the contact angle is denoted by $\phi$. Simple geometric relations exist between the bubble radius, the bubble height, the contact angle and the cavity mouth radius.

Figure 3.4 graphically depicts Hsu's criterion for onset of nucleate boiling. The condition for nucleation of a stable vapor bubble is obtained based on the interaction of the curve depicting Equation 3.8 and the linear temperature profile of the liquid in the superheated near-wall region. The critical mouth radius of a cavity that can be a potential nucleation site for the onset of nucleate boiling, is obtained at the point of tangency between the local temperature profile and the curve representing Equation 3.8. This critical cavity mouth radius is indicated as $r_{crit}$ in Figure 3.4. For any increase in input heat, leading to an increase in temperature of the superheated liquid layer, a range of cavities become potential nucleation sites and the mouth radius of these cavities is limited by the in-

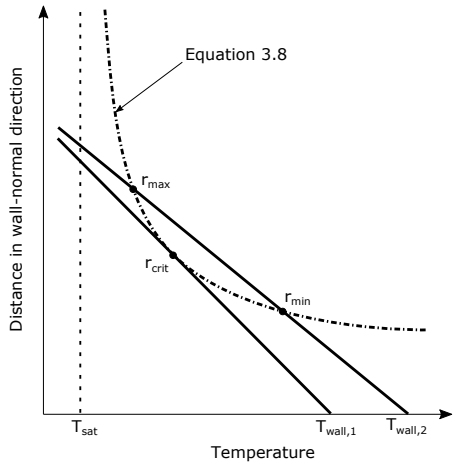


Figure 3.4: *Criterion for the onset of nucleate boiling.*

tercepts indicated by $r_{min}$ and $r_{max}$ in Figure 3.4. Cavities smaller than $r_{min}$ require higher superheat for nucleation and cavities larger than $r_{max}$ experience condensation at the bubble tip, preventing the existence of a stable vapor nucleus. However, it should be noted that even if the required superheat conditions are satisfied, a cavity becomes an active nucleation site only if it contains a vapor embryo, in other words, if it is not completely flooded by the liquid [17]. In essence, Hsu's criterion [18] relates the thickness of the superheated liquid layer to the cavity sizes on the heated surface to obtain an analytical expression for onset of nucleate boiling. Sato and Matsumura [19] obtained a similar criterion for onset of nucleate boiling in forced convection boiling. The expression for superheat at onset of boiling, $\Delta T_{sat,ONB}$, based on Sato and Matsumura's criterion [19] for forced convection boiling reads,

$$\Delta T_{sat,ONB} = \frac{4\sigma T_{sat} v_{lv} h_{conv}}{k_l h_{lv}} \left[ 1 + \sqrt{1 + \frac{k_L h_{lv} \Delta T_{sub}}{2\sigma T_{sat} v_{lv} h_{fc}}} \right] \tag{3.9}$$

where $h_{fc}$ is the single phase forced convection heat transfer coefficient, $v_{lv}$ is the difference between the specific volumes of the vapor and the liquid and $k_l$ is the thermal conductivity of the liquid.

## 3.4 Factors influencing boiling

As discussed previously, nucleate boiling is a complicated phenomenon with multiple thermal and mechanical interactions between the phases. Hence boiling is influenced by several factors pertaining to the liquid, the vapor and the solid material. Moreover, the

effect of these factors vary depending on the boiling regime in subcooled boiling flow. These factors and their effects are discussed in detail in this section.

The factors influencing nucleate boiling, which are extensively discussed in the literature, are listed below and are discussed in detail subsequently.

- Coolant flow rate
- Coolant subcooling
- System pressure
- Material of the heated solid
- Surface characteristics of the heated solid
- Composition of the liquid coolant
- Orientation of the heated surface
- Vibration
- Other factors...

### 3.4.1 Coolant flow rate

In the single phase forced convection regime, an increase in coolant flow rate or the bulk velocity of the coolant results in increased heat transfer. With regard to nucleate boiling, higher coolant velocity delays the onset of nucleate boiling. The onset of nucleate boiling is characterised by the existence of a stable vapor bubble, for which a superheated liquid surrounding is essential. For an increase in coolant velocity, the thinner thermal boundary layer on account of a thinner velocity boundary layer results in a thinner superheated liquid layer close to the wall. This prevents the existence of a stable vapor bubble. A higher wall superheat is required to increase the thickness of the superheated liquid layer and thereby for the onset of bubble nucleation. Campbell [20] postulated that for very high coolant flow rates, the flow may suppress and overwhelm bubble initiation and growth. Lee and O'Niel [21], within the operating range of their experiments, observed complete suppression of nucleate boiling with increase in coolant velocity beyond a certain value. In the partial boiling regime, the higher coolant velocity results in boiling suppression. The inertial forces of the flow displace a growing vapor bubble prematurely from its nucleation site. This is known as flow induced suppression of nucleate boiling [22]. Furthermore, in the fully developed boiling regime, the heated surface is covered by bubble nucleation sites, which overwhelms the convective boundary layer. Thereby, as mentioned previously, the heat transfer mechanism is similar to that in pool boiling. Under such circumstances, the boiling curves corresponding to different coolant velocities merge into the pool boiling curve. Beyond the fully developed boiling regime, the critical

heat flux is a strong function of the coolant velocity and the higher the coolant velocity, the higher the critical heat flux. Finally, the net vapor generated in the system is also a function of the coolant flow rate and it increases with decrease in coolant flow rate.

### 3.4.2 Coolant subcooling

Subcooling is defined as the difference between the saturation temperature of the coolant, at a given operating pressure, and the coolant bulk temperature. In the single phase forced convection regime, an increase in coolant subcooling or a decrease in its bulk temperature results in an increase in heat transfer. This is due to the greater potential for heat transfer on account of higher temperature difference between the heated wall and the liquid bulk. Lower bulk temperature also results in a thinner superheated liquid layer close to the wall. Thereby, an increase in subcooling prevents the existence of a stable vapor bubble and a higher wall superheat is required for onset of nucleate boiling. In the partial boiling regime, an increase in subcooling, on the one hand, results in increase in heat transfer as the colder liquid from the bulk quenches the hot surface after bubble detachment. The higher the subcooling, the higher the quenching effect which entails a higher heat transfer rate. On the other hand, a colder liquid bulk causes suppression of nucleate boiling. A vapor bubble growing in size due to evaporation of the liquid micro-layer close to the heated surface, experiences a simultaneous condensation at its tip, which is away from the heated surface and in contact with the liquid bulk. This is known as subcooling-induced suppression of nucleate boiling[22]. The higher the subcooling the higher the suppression. Similar to the effect of coolant velocity, the subcooling has little or no influence on the fully developed boiling regime as evidenced by experimental data [17]. Furthermore, the critical heat flux increases with increase in the subcooling.

In practical applications, such as internal combustion engines, the bulk coolant temperature at the inlet is set to a particular value. The heat transfer rate in any specific location depends on the local coolant temperature. The local coolant temperature depends on the conditions upstream and also on the coolant flow rate. A decrease in the coolant flow rate, keeping its bulk temperature at inlet constant, results in an overall increase in the coolant temperature inside the coolant jacket. Also, the net vapor generated in the system increases with decrease in coolant subcooling.

### 3.4.3 System pressure

The operating pressure of the cooling system does not affect the initial single phase forced convection regime, since the liquid coolant is nearly incompressible. The liquid saturation temperature increases with increase in system pressure. So, the temperature for the onset of nucleate boiling increases with increase in system pressure. Based on the theory of vapor bubble formation and growth, it is evident that for a given liquid superheat, an increase in system pressure results in a smaller vapor bubble radius, as given

in Equation 3.8. With increasing pressure, higher thermal energy is required to generate and grow vapor bubbles [20]. An increase in system pressure also results in an increase in critical heat flux. It is worth noting that, increasing the system pressure, keeping the coolant bulk temperature constant, means increased coolant subcooling. Due to this increased subcooling, the net vapor generated in the system decreases with increasing pressure. Lee and O'Niel [21], in their experiments, increased the system pressure and the coolant bulk temperature simultaneously in order to ensure constant subcooling. This way they decoupled the effects of system pressure from that of subcooling. They observed insignificant changes in net vapor generated with increase in system pressure when the subcooling was kept constant. They concluded that vapor entrainment can be controlled by subcooling, but not by system pressure.

### 3.4.4 Material of the heated solid

The thermophysical properties of the heated solid influences the boiling heat transfer. Local heat transfer by conduction within the solid in the vicinity of the nucleation site occurs due to the following physical mechanisms.

- **Vapor bubble growth**: A growing vapor bubble attached to its nucleation site, continues to grow as a result of heat transfer from the surrounding superheated liquid layer. A significant amount of energy is required for this phase change process on account of the latent heat of vaporization. This energy is supplied to the superheated liquid layer at the heated surface in the vicinity of the nucleation site. So, the temperature close to the nucleation site drops and thereby results in heat transfer by conduction from the neighbouring warmer regions within the solid.
- **Waiting period**: The time between the departure of one vapor bubble and nucleation of the next bubble at a nucleation site is known as the waiting period. After a bubble is detached from its nucleation site, the site is cooled by surface quenching and the temperature in the location drops below the critical temperature required for bubble nucleation. Heat is then transferred towards the region of the nucleation site from the surrounding warmer regions, resulting in a local transient conduction within the heated solid. Through this local transient conduction process, enough heat is recovered by the nucleation site in order to recreate the superheated liquid layer required for the nucleation of another stable vapor bubble.

Several studies [23–25], both experimental and numerical, have discussed the effect of thermophysical properties of the solid surface on heat transfer, both during bubble growth and the waiting period. Aktinol and Dhir [23] did a numerical study on a single vapor bubble on a heated surface with different materials. They concluded that boiling on heaters with higher thermal conductivity and diffusivity resulted in lower waiting time, slower growth rate and smaller bubbles. Zou and Jones [26, 27] studied the influence of thermal conductivity of the hot solid on the nucleation site density and interaction

between nucleation sites by boiling the liquid R134A on copper and stainless steel surfaces. They found that materials with higher thermal conductivity had more uniform spatial distribution of nucleation sites and larger area of influence (with lower wall temperature) around the nucleation site. French [28] observed significantly higher wall superheat on 'as-cast' surfaces of cast iron test specimens, compared with that on a copper specimen. An 'as-cast' surface is the surface of the specimen that is in contact with the sand core during the casting process and in contact with the coolant in the experiments. Furthermore, among the cast iron specimens, French observed that the wall superheat is higher for a specimen with an 'as-cast' surface compared to a machined surface. In line with this, French specified that there exists a thermal barrier to heat transfer when boiling occurs on the as-cast surface of a cast iron specimen. French further quantified this effect using a thermal barrier index and correlated it with the eutectic cell size, a parameter related to the casting process.

### 3.4.5 Surface characteristics of the heated solid

The microgeometry of a surface is characterised by surface elements, such as plateaus, valleys, peaks, crevices, cavities, etc. It is extremely difficult to quantify these surface elements for surfaces used in practical applications, like those in passages of the engine coolant jacket. The average roughness height, $R_a$, is generally used to quantify the roughness of such surfaces. The average roughness height is the arithmetic average of absolute values of surface deviations from a mean line. On the one hand, an increase in surface roughness, i.e., a higher values of $R_a$, usually results in an increase in single phase heat transfer rate mainly due to (a) increase in surface area for heat transfer and (b) change in turbulence pattern close to the wall caused by the roughness [29]. On the other hand, the effect of the surface roughness on nucleate boiling is more complex. It is impossible to mathematically describe bubble nucleation on surfaces used in practical applications in a deterministic way [15]. Therefore, a number of studies have focused on correlating the wall heat flux from subcooled boiling flow with the average roughness height, $R_a$, of the surface. Robinson [29] investigated aluminium alloy test specimens with different surface roughness, quantified by $R_a$. An 'as-cast' surface with $R_a = 14.20\mu m$ and a 'smooth' surface with $R_a = 0.345\mu m$ were tested. Robinson reported that the heat transfer rate in the 'as-cast' surface was higher during single phase forced convection, however, the increase in heat transfer rate due to increase in surface roughness was much lower once boiling was established. Campbell et al. [30] studied the effect of surface roughness on subcooled boiling flow on surfaces with three different values of $R_a$, a 'smooth' surface with $R_a = 0.3\mu m$, an 'intermediate' surface with $R_a = 0.9\mu m$ and an 'as-cast' surface with $R_a = 9.1\mu m$. They observed the 'as-cast' surface experienced onset of boiling at a lower surface temperature and also experienced higher heat transfer rates compared to the other two surfaces. They also observed that the tests were not repeatable in the nucleate boiling regime and the boiling curves drifted towards higher wall superheats with ageing. This drift was attributed to deposits on the heated surface and coolant contamination. Breitschädel [31], reported by Steiner et al. [15], studied the effect of surface roughness together with the effects of surface ageing on subcooled

boiling flow on aluminium samples, in conditions similar to automotive cooling. The surfaces considered were 'smooth' with $R_a = 2\mu m$, 'standard' with $R_a = 45.7\mu m$ and 'rough' with $R_a = 130\mu m$. The studies indicated that both the smooth and the rough surfaces experienced degradation of heat transfer rate with time (ageing), shifting the respective boiling curves towards higher wall superheats. This degradation was attributed to deactivation of initially active nucleation sites and the boiling curves corresponding to the smooth and rough surfaces approached the boiling curve of 'long-term measurement' of 2000 hours using the standard surface.

Although $R_a$ is representative of the average surface roughness, it is a crude representation and does not give any information regarding the relationship between the microgeometry and the active nucleation sites, which is the most important aspect in nucleate boiling. Steiner et al. [15] state that it is impossible to mathematically describe the bubble nucleation process on a 'real life technical surface' in a deterministic way. They further explained the effects of surface roughness on nucleate boiling heat transfer by stating that an increase in surface roughness will result in higher heat transfer rate only if the increased roughness translates to additional active and stable nucleation sites.

### 3.4.6 Composition of the liquid coolant

The coolant used in most automotive engines consists of two components, water and ethylene-glycol. The coolant is usually a 50/50 Vol% mixture of these components. Ethylene-glycol has anti-freeze properties and therefore brings the freezing point of the aqueous solution down, enabling the usage of the coolant in cold climates. Out of the two components, water has a lower saturation temperature and is, therefore, more volatile. Robinson [29] experimentally studied the effect of composition of the liquid coolant by testing three different coolants: pure water, pure antifreeze (93% ethylene-glycol + additives) and a 50/50 Vol% aqueous solution of antifreeze. The highest heat transfer rate was obtained with pure water and the lowest with pure antifreeze. The heat transfer rate obtained using the 50/50 Vol% aqueous solution was in between these extremes. The higher heat transfer rate obtained using pure water was attributed to its lower viscosity and higher thermal conductivity in the convection regime. The lower saturation temperature and lower surface tension of water were credited for its superior heat transfer characteristics in the nucleate boiling regime. Breitschädel [31], reported by Steiner et al. [15], studied the effect of coolant composition by varying the proportion of ethylene-glycol in the aqueous solution. The proportions, 40/60, 50/50 and 60/40 Vol% of ethylene-glycol/water were considered. Similar to conclusions of Robinson [29], the results confirmed the higher the proportion of ethylene-glycol, the lower the heat transfer rate. The difference in volatility between the two components causes the liquid close to the nucleating surface to be rich in the less volatile component, i.e., ethylene-glycol. This non-azeotropic effect increases the effective saturation temperature of the local mixture, resulting in a decrease in heat transfer rate. Steiner et al. [32] numerically modelled these cases using the Boiling Departure Lift-off (BDL) model. They concluded that it was sufficient to consider the binary coolant mixture as an azeotropic mixture

in order to model the effects of varying the ethylene-glycol/water ratio in the aqueous solution without significant loss of accuracy. Also, Campbell [20], while discussing about the fluid properties of the binary mixture of ethylene-glycol and water, suggests to use values corresponding to water for properties such as surface tension, vapor density and latent heat of vaporization. This is justified since water is more volatile compared with ethylene-glycol, and is therefore assumed to be the dominant component in the vapor [20].

### 3.4.7 Orientation of the heated surface

The ratio of liquid to vapor density in nucleate boiling of an aqueous solution, such as that of ethylene-glycol, is quite high. Thereby, the conditions in the thermal boundary layer close to the heated wall are influenced by the buoyancy force. Consequently, the orientation of the heated surface with respect to the direction of gravitational acceleration becomes an important factor that affects the vapor bubble dynamics and, therefore, the heat transfer rate in the nucleate boiling regime. Several experimental studies [32–35] have reported the effect of orientation of the heated surface on heat transfer in subcooled boiling flow. It was inferred that for a downward facing heated surface, low values of bulk flow velocity result in rapid increase in wall temperature for a given wall heat flux. When the bulk flow velocity is high, independent of the orientation of the heated surface, the growing vapor bubbles are detached from their respective nucleation sites and are convected by the flow due to the high inertial forces of the flow itself. However, when the velocity is low, the dynamics of the vapor bubbles are dominated by the buoyancy force. For a downward facing heated surface, the buoyancy force keeps the vapor bubbles close to the heated surface, leading to coalescence and agglomeration of vapor bubbles in the vicinity of the heated surface. Consequently, a partial vapor film is formed that impedes heat transfer, thus lowering the heat transfer rate and also the critical heat flux.

### 3.4.8 Vibration

Vibration is an inevitable part of engine operation. Therefore, it is relevant to understand the effect of vibration on the nucleate boiling heat transfer. Robinson [29] and Steiner et al. [32] experimentally studied the effect of vibration (of the heated surface) on the heat transfer rate in subcooled boiling flow and arrived at similar conclusions. Steiner et al. [32] conducted experiments at a system pressure of $1.2bar$ and found a very small difference in heat transfer rate between the vibrating and non-vibrating configurations, also for a bulk velocity as low as $0.05m/s$. Robinson [29] investigated the effect of vibration at different operating pressures and coolant flow velocities. Robinson inferred that vibration causes an increase in heat transfer rate for low coolant flow velocity and low system pressure, but has negligible effects for increasing velocity and system pressure. Both Robinson [29] and Steiner et al. [32] concluded that for conditions relevant to that in internal combustion engines, the effect of vibration could be neglected.

### 3.4.9 Other factors

In addition to these factors, there are other factors that also influence the nucleate boiling heat transfer. These include the presence of dissolved gases in the liquid coolant, additives added to the coolant (such as the ones for corrosion prevention), coolant contamination, deposits on the heated surface, etc.

The discussions in this section further emphasise the complexities involved in subcooled boiling flow and the strong need for dedicated experimental and numerical investigations to gain deeper insights into this complex phenomenon.

# 4

# Experimental and numerical studies: a brief review

The fundamental physical mechanisms involved in nucleate boiling are challenging to analyse and understand directly from practical applications with liquid cooling, such as internal combustion engines, electronic chips, exhaust gas recirculation system and the like. The challenges could be due to various reasons including, but not limited to, lack of access for measurement probes, lack of visual access, cost and expertise required to test such applications, interactions with other subsystems and lack of possibility to isolate the phenomenon being analysed. In order to overcome these difficulties, experiments aimed at understanding the fundamental physical mechanisms involve simple geometries, often representative of the conditions in the practical application of interest, with a visually accessible boiling surface. In addition to offering the possibility to understand the phenomenon of nucleate boiling, these experiments also provide valuable data for development and validation of numerical boiling models. Several empirical and semi-mechanistic numerical models have been developed based on data from such experimental investigations. This chapter presents a brief review of the experimental and numerical studies in subcooled boiling flow, specifically relevant to cooling of internal combustion engines.

## 4.1 Experiments investigations

The region between the two exhaust valves, knows as the exhaust valve bridge, in an engine cylinder head is usually among the most critical regions. This is because the region experiences high thermal loads due to the in-cylinder combustion and the heat rejected from the exhaust valve seats. Such a region is shown in Figure 4.1. Therefore, in general, the experimental studies relevant to engine cooling are designed to be representative of the conditions in region of the exhaust valve bridge. Such experiments involve the flow of coolant in a channel with the heated surface mounted flush with the bottom face of the channel. There are a number of experimental studies on subcooled boiling flow related to engine cooling. This chapter presents a review of some of the recent experimental studies.

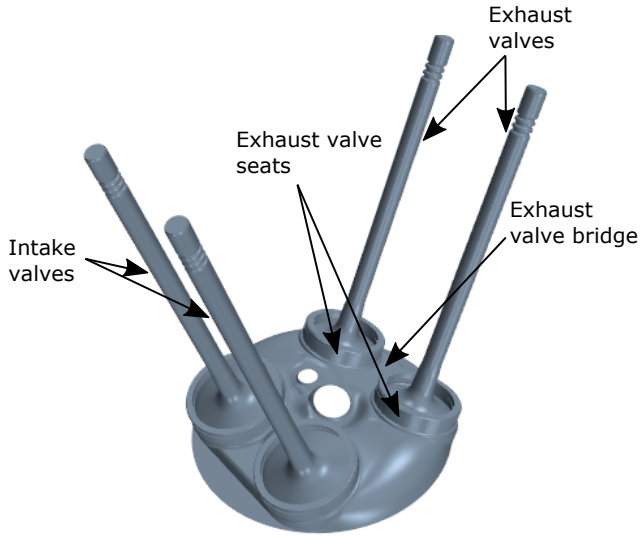


Figure 4.1: *Example of geometry of the flame deck showing the intake valves, exhaust valves, exhaust valve seats and the exhaust valve bridge region.*

Robinson [29] studied the heat transfer in the forced convection and nucleate boiling regimes experimentally and correlated the data with numerical models. The test section was a rectangular channel with a width of $16mm$ and had a provision to adjust its height. The test specimen was made of AS10G aluminium alloy, which is generally used in cylinder head casting. The coolants used were pure distilled water, pure antifreeze (with 93% ethylene glycol+additives), 50-50 Vol% mixture of distilled water and antifreeze and 50-50 Vol% mixture of distilled water and 'Blue' hybrid coolant. Operating parameters such as coolant flow rate, system pressure and coolant bulk temperature at the inlet were varied in the tests. Additionally, the effects of varying channel height, surface roughness of the specimen and coolant type were also included in the tests. Furthermore, the test section was linked to a shaker in order to analyse the effects of vibration. The data from the test rig resulted in an extensive database relevant to heat transfer in the coolant jacket of internal combustion engines.

Campbell [30] studied subcooled boiling flow, experimentally, using a rectangular channel. The channel was $10mm$ in width with a rectangular test specimen mounted at its bottom face. The height of the channel could be varied in order to study the effects of change in hydraulic diameter. The test specimens were made of copper and aluminium alloy A319. A coolant with 50-50 Vol% mixture of ethylene glycol and water was used. Coolant flow rate, system pressure, coolant bulk temperature at the inlet and channel height were varied during the tests. For certain flow and thermal conditions, the critical heat flux limit was attained and the results for those conditions were also presented. In addition to these, test results analysing the effects of aging, hysteresis and repeatability were also

presented. Campbell [20] also developed a systematic approach for processing the data, both in the forced convection and the nucleate boiling regimes, in order to analyse the test results in line with the theory of subcooled boiling flow.

Steiner et al. [22] studied experimentally the phenomenon of subcooled boiling flow of water on an aluminum alloy test specimen. The test section was a rectangular-sectioned channel, $30mm$ in width and $40mm$ in height. The rectangular test specimen was mounted on the bottom face of the channel. The system pressure and flow rate were varied during the tests. The results from the tests were also used to validate the BDL numerical boiling model. In another experimental campaign in a channel flow with square cross section ($36mm \times 36mm$), Steiner et al. [32] studied extensively the sensitivity of the boiling phenomenon to several parameters, such as composition of the liquid coolant (varying proportions of water and ethylene glycol antifreeze), roughness of the heated surface and orientation of the heated surface. In these studies, they also investigated the effect of vibration on boiling heat transfer rate. The test specimen was made of aluminium alloy and the liquid coolant used was a mixture of water and ethylene glycol. Major inferences from this study were that the non-azeotropic effects could be neglected while specifying coolant properties, the surface roughness (in terms of roughness height) has almost negligible effect on heat transfer rate when long-term operation is considered, downward facing heated surfaces with low bulk velocity experienced transition to 'partial film boiling' at low wall superheats and the effects of vibrations on heat transfer were observed only at low bulk velocities. Furthermore, the BDL model was evaluated with the results from the experiments.

Kandlikar and Bulut [36] studied, experimentally, the effect of varying proportions of ethylene glycol in water mixture. The rectangular-sectioned channel used was $40mm$ wide and $3mm$ high. The test specimen, made of aluminium, was cylindrical with a diameter of $9.5mm$. The circular surface of the specimen was placed centrally on the $40mm$ side of the channel. The mass fraction of ethylene glycol in water was varied from 1% to 40%. They observed that the heat transfer deteriorated with increase in proportion of ethylene glycol. This deterioration was attributed the mass diffusion effect, caused by the increase in concentration of the less volatile ethylene glycol in the near-wall region, where the vapor bubbles were generated. The Kandlikar's model [37] was modified to account for the effects of the binary mixture and was validated with the experimental results. In doing so, three regions were identified, based on mass fraction of ethylene-glycol, to describe the mixture effects: the 'near-azeotropic' region where the mass diffusion effects are negligible, the 'moderate suppression' region and the 'severe suppression' region where the effects of mass diffusion progressively suppressed nucleate boiling. Accordingly, a suppression factor, accounting for the mass diffusion effect, was introduced in the numerical model.

Lee and O'Niel[21] made their experiments on a rectangular-sectioned channel flow with a copper heater at its bottom face. They studied the difference in boiling characteristics between water and a 50-50 Vol% mixture of water and ethylene glycol. The channel was $30mm$ in width and $20mm$ in height. For both coolants, boiling curves were obtained by varying the coolant flow rate, system pressure and the coolant bulk temperature at the

inlet. Photographic evidence of the boiling surface under different operating conditions were presented and also used to understand the physics. They observed that the vapor bubbles were smaller in water compared with the mixture, especially when the liquid subcooling was high. They also inferred that vapor entrainment at high heat fluxes could be controlled with liquid subcooling, but not with system pressure for both coolants.

Hua et al. [38] and Abou-Ziyan[39] studied subcooled boiling flow of water on cast-iron test specimens. While Hua et al. [38] made their investigation in a rectangular cross-section channel, Abou-Ziyan [39] used a T-shaped cross-section channel, which was considered to be more representative of the exhaust-valve bridge region of the engine cylinder head. While the former varied the operating conditions, such as coolant flow rate, system pressure and coolant bulk temperature at the inlet, the latter studied the effect of different aspect ratios corresponding to the dimensions of the T-section. High wall superheats, in the order of $80 - 100°C$, were attained in the tests with cast-iron specimens. This could be attributed to the thermal barrier effect observed by French [28] in cast-iron specimens. Abou-Ziyan [39] removed, as a preparatory step, $1.5mm$ of material from the 'as-cast' surface of the specimen in order to negate this thermal barrier effect. However, it is difficult to conclude if the thermal barrier effects were completely negated, since results with the thermal barrier while boiling on the 'as-cast' surface, i.e., before removing the material, are not available.

Other recent experiments in subcooled boiling flow include the ones by Paz et al. [35] and Torregrosa et al. [40]. In addition to experiments of the kind reviewed so far, there have been experimental studies focusing on very specific physical mechanisms involved in boiling, such as bubble nucleation, growth and detachment [41–43], distribution and density of nucleation sites [26, 44–46], interaction between nucleation sites [16, 47–49] and the like.

As mentioned previously, experimental investigations help us to better understand the phenomenon of nucleate boiling and the physical mechanisms associated with it. Furthermore, the insights gained and the database generated from these experiments also provide a platform for development and validation of empirical and semi-mechanistic numerical boiling models.

## 4.2 Numerical modelling

Subcooled boiling flow involves heat transfer by both forced convection and nucleate boiling. Therefore, heat flux partitioning is the preferred approach for numerical modelling. In the heat flux partitioning approach, the total wall heat flux is expressed as a superposition of the forced convection and the nucleate boiling components. A simple implementation of the heat flux partitioning approach was presented by Bo [50]. In his calculations, a simple superposition model of the convective heat flux, obtained from Computational Fluid Dynamnics (CFD) simulations, and nucleate boiling heat flux,

obtained from Rohsenow's correlation [51] was used. A number of other established numerical boiling models have been proposed based on the heat flux partitioning approach with varying levels of empiricism. As mentioned previously, subcooled boiling flow is a complicated phenomenon influenced by several factors, with certain characteristics that can not be quantified. Hence, development of numerical models with empiricism and empirical constants is inevitable. While some numerical models use a complete empirical formulation for wall heat flux modelling to account for such effects, other models use a mechanistic approach which is based on one or a few dominant physical mechanisms. However, models based on a mechanistic approach involve a fair level of empiricism in the sub-models used. A brief review of certain numerical models that use the aforementioned approaches is presented below.

Kandlikar [37] developed a boiling model by employing different correlations for the forced convection, partial boiling and FDB regimes. Heat transfer in the forced convection regime was modelled using Petukhov's correlations [52]. The heat flux in the partial boiling regime was expressed using a power law of wall superheat and the heat flux in the FDB regime was expressed using a boiling number based correlation. The point of intersection of the forced convection curve and the FDB curve was identified and the heat flux at this point was multiplied by 1.4 to obtain the heat flux at the transition between the partial boiling and FDB regimes. This method of identifying the transition from partial boiling to FDB was earlier used by Bowring [53]. Shah [54] also used a similar approach, in which the correlation was based on the boiling number. However, the Kandlikar's model estimates the boiling heat flux more accurately, compared with Shah's model, in both the partial boiling regime and the FDB regime [37]. Prodanovic et al. [55] also used a similar method in their boiling model.

Chen [56] developed a boiling model using the heat flux partitioning approach and, in addition, accounted for the enhancement of forced convection due to presence of vapor bubbles, $F$, and suppression of nucleate boiling due to forced flow, $S$. The model formulation reads,

$$q_{wall} = Fq_{fc} + Sq_{nb}. \tag{4.1}$$

The forced convection component, $q_{fc}$, is estimated using Dittus-Boelter correlation [57] and the nucleate boiling component, $q_{nb}$ is estimated using Foster and Zuber's correlation [58]. Although Chen's model was developed for saturated flow with net vapor generation, the formulation is applicable for subcooled flow conditions with minor modifications. The suppression factor, $S$, in Chen's model is calculated using Reynolds number of the bulk flow. The Boiling Departure Lift-off (BDL) model, presented by Steiner et al. [22], improved Chen's model by estimating the suppression factor, $S$, based on local parameters in the flow instead of bulk parameters. In the BDL model, the suppression factor is based on a mechanistic formulation and is expressed as a product of a flow-induced suppression, $S_{flow}$ and a subcooling induced suppression, $S_{subcool}$. The flow-induced suppression accounts for the mechanism observed by Klausner et al. [43] and Steiner et al. [15] in their own experiments. The mechanism is described as follows: The inertial forces of the forced flow cases a premature detachment of a growing vapor bubble from its nucleation site.

The detached bubble is convected by the flow, while it continues to grow. As the bubble grows to a certain size, it rises into the liquid bulk as a result of increased buoyancy. The subcooling-induced suppression, $S_{subcool}$, accounts for the condensation, occurring at the bubble tip which is in contact with the subcooled liquid bulk. The formulation of $S_{subcool}$ is based on the concept of 'extrapolated superheat layer thickness' [22].

Kurul and Podowski [59] proposed the Rensselaer Polytechnic Institute (RPI) wall boiling model which is also based on the heat flux partitioning approach, however, with a more mechanistic formulation of the same. The expression for the total wall heat flux in the RPI model reads,

$$q_{wall} = q_{fc} + q_q + q_e \tag{4.2}$$

where $q_{fc}$ represents the single phase convective heat flux, $q_q$ and $q_e$ represent the heat flux due to quenching and evaporation, respectively. The formulation of these individual components account for several physical parameters related to subcooled boiling flow, such as bubble diameter, bubble nucleation frequency, bubble nucleation site density and area covered by nucleating vapor bubbles.

Conventional engine cooling systems are designed for heat transfer by forced convection. When the inadvertent occurrence of nucleate boiling, in critical regions like the exhaust valve bridge, was realized, the coolant passages were redesigned to either suppress the boiling or keep it to a minimum level. In line with such an approach, a numerical wall boiling model was expected to capture the occurrence of nucleate boiling and estimate the boiling heat flux. Therefore, empirical correlations, such as Rohsenows correlation [51] or semi-mechanistic models like the Chens model [56] and the BDL model [22] were successfully implemented in analysis of heat transfer in the engine coolant jacket [50, 60–62]. However, in modern day engines with higher specific power, and consequent higher thermal load, boiling suppression becomes more difficult. Also, the potential of controlled local nucleate boiling as a viable option for precision cooling has been well established. In line with this, the role of a boiling model in the numerical analysis of heat transfer in the engine coolant jacket has become more significant. In addition to predicting the occurrence of local nucleate boiling and estimating the associated wall heat flux, the boiling model is also expected to estimate the extent of boiling in order to avoid the critical heat flux and eventually transition and film boiling. Thereby, boiling models that account for increase in vapor bubble population and the resulting influence on the wall heat flux are sought for. For example, the RPI model [59] accounts for the vapor bubble population and the area of the heated surface covered by vapor bubbles using the active nucleation site density. The model has been used in analysis of heat transfer in the engine coolant jacket [63, 64].

A new blended boiling model is proposed by the author. The model blends two well established boiling models in the literature. Additionally, the model accounts for vapor bubble interactions using a semi-mechanistic approach, which in turn provides information about the extent of boiling. A summary of the model is reported in the following chapter. A thorough presentation of the model and its formulation can be found in Paper A in the appendix.

# 5

# Summary of contributions

The contributions of the author, in line with the aims of the thesis, are presented in this chapter. The contributions include the following:

1. **Paper A**: Development and validation of the proposed wall boiling model.
2. **Paper B**: A detailed thermal survey measurement campaign of a four-cylinder petrol engine, focusing on boiling in the coolant jacket.
3. **Paper C**: Implementation of the boiling model, presented in Paper A, in a Computational Fluid Dynamics - Conjugate Heat Transfer (CFD-CHT) simulation of the four cylinder petrol engine and model evaluation with measurements.
4. **Paper D**: A comparative analysis of single phase and multiphase CFD frameworks for analysing subcooled boiling flow.
5. **Paper E**: Design and construction of a boiling rig.

The key features of each of the contributions are highlighted in the subsequent parts of this chapter. However, the reader is referred to the relevant scientific articles, available in Part II of this thesis, for more details.

## 5.1 Paper A : The Blended Boiling Model

Paper A, by Vasudevan et al. [1], presents the formulation of the Blended Boiling Model, BBM, and the model validation with experiments from the literature. The model estimates the wall heat flux in subcooled boiling flow by combining two well established wall boiling models in the literature, the BDL model presented by Steiner et al. [22] and the pool boiling correlation proposed by Rohsenow [51]. On the one hand, the BDL model is intended to estimate the wall heat flux in the isolated bubbles regime, where the surrounding subcooled liquid flow is unaffected by the presence of the bubbles. The model is developed based on the balance of forces acting on an isolated vapor bubble. While the accuracy of the BDL model is remarkably good in the partial boiling regime, the

model predictions deviate significantly from the experimental results in the FDB regime, especially for low values of bulk flow velocity. This is attributed to the complex bubble-bubble interactions and the two-way coupling between the dynamics of multiple vapor bubbles and the liquid bulk flow. Since the BDL model is developed based on dynamics of an isolated vapor bubble, the effect of multiple interacting bubbles and their influence on the bulk flow is not accounted for [22]. On the other hand, the Rohsenow's correlation [51] is developed empirically to estimate the wall heat flux in pool boiling. Since the mechanism of heat transfer occurring in the FDB regime in a subcooled boiling flow is quite similar to that of pool boiling, the Rohsenow's correlation could be used in the FDB regime. The Blended Boiling Model, BBM, using a semi-mechanistic formulation blends the BDL model and Rohsenow's correlation in order to estimate the total wall heat flux. Additionally, the BBM suggests a modification to the formulations of the drag and lift forces in the BDL model. The two key highlights of the BBM are given below.

- **Modified formulation of drag and lift forces in the BDL model**
  In the BDL model, formulations for the drag and lift forces are based on an isolated bubble in an unbounded flow field. However, in case of nucleate boiling, the bubbles nucleate on the surface of the wall and the presence of the wall significantly influences the drag and lift forces acting on a bubble. So, in the BBM, the formulations of the drag and lift forces proposed in the original BDL model are replaced with the ones proposed by Mazzocco et al. [65], which accounts for the presence of the wall. Consequently the agreement of the model predictions with experimental results improved, without having to modify the empirical constants in the formulation of the original BDL model presented by Steiner et al. [15].

- **Blending two wall boiling models**
  As mentioned previously, the BDL model estimates the wall heat flux in the isolated bubbles regime and the Rohsenow's pool boiling correlation is applicable in the FDB regime. The difference between the two regimes is characterized by an increase in vapor bubble population and their interactions. In the BBM, a semi-mechanistic formulation is proposed that accounts for the increase in bubble population and their interaction. The formulation is based on the number of active bubble nucleation sites and their distribution on the heated surface. On account of this the probability of bubble interaction is introduced as a parameter that weighs the relative importance of the BDL model and the Rohsenow's correlation.

The expression for the wall heat flux estimated by BBM reads,

$$q_{BBM} = (1 - \Pi) q_{BDL} + \Pi q_{Roh}; \quad 0 \leq \Pi \leq 1 \tag{5.1}$$

Notably, the expression for $q_{wall}$ consists of three components: the heat flux, $q_{BDL}$, estimated using the BDL model, the heat flux, $q_{Roh}$, estimated using the Rohsenow's correlation and the probability of bubble interaction, $\Pi$. In the BBM, $\Pi$ denotes the probability of occurrence of more than one vapor bubble nucleation site within a circular area with a diameter twice that of the bubble diameter, which in turn indicates bubble

interaction. The value of $\Pi = 1$ is interpreted as FDB regime and the wall heat flux is estimated only using the Rohsenow's correlation, as evident from Equation 5.1. Although the model does not give any information regarding the critical heat flux or the transition and film boiling regimes, the value of $\Pi$ is suggested to be used as a parameter to determine the extent of boiling. In practical applications, such as the engine coolant jacket, operating within the partial boiling regime, with minimal net vapor generation is beneficial. Although operating in the FDB regime contributes to an increase in heat transfer rate, the margin to encounter critical heat flux and eventually transition and film boiling regimes is quite small. Therefore, the value of $\Pi$ is suggested to be used as a parameter to estimate the extent of boiling and to limit the operation within the partial boiling regime for practical engineering applications. The model has been validated with data from two experiments using different materials for the heated solid, Aluminium alloy and Copper. The model estimates the wall boiling heat flux that is in reasonably good agreement with the experiments. Nucleate boiling on cast iron is of interest to the heavy-duty automotive and marine engine manufacturers. Experimental evidence of high wall superheats in cast-iron specimens and the limitations of the blended model in capturing this has also been discussed briefly in Paper A. The possibility of correlating the thermophysical properties of the metal in the boiling model is also mentioned.

However, based on the findings of French [28], it is evident that the thermal barrier effect in cast-iron is the reason for this high wall superheats encountered and this is not included in Paper A. Further investigation into the thermal barrier effect and accounting for this resistance to heat transfer in the boiling model is an interesting work for the future.

## 5.2 Paper B: Thermal survey measurement campaign on a four-cylinder petrol engine

Measurements are conducted on a four-cylinder Volvo passenger car petrol engine, commonly known as Volvo Engine Petrol (VEP), mounted in a test cell with necessary instrumentation. The engine-driven mechanical pump is replaced with an electric pump, so that the coolant flow rate can be set arbitrarily. Thermocouples were placed in several locations of the engine cylinder head and in the coolant flow passages. Parameters such as the operating pressure of the cooling system, the coolant flow rate and the bulk temperature of the coolant at the inlet, are varied systematically and the temperatures at several chosen locations of the engine are recorded. The measurements are conducted for the maximum torque and maximum power operating load points. Moreover, based on the data available from the tests, inaccuracies in temperature measurement due to the uncertainty in probe placement are quantified. Paper B presents the results from this detailed systematic measurement campaign, analysed in line with the theory of subcooled boiling flow in two critical locations in the engine coolant jacket: the exhaust valve bridge and in the vicinity of the exhaust flange in the Integrated Exhaust Manifold (IEM). The key findings based on the thermal survey measurement campaign are presented below.

- Decrease in system pressure, decrease in coolant flow rate and increase in bulk temperature of the coolant resulted in increase in heat transfer rate due to boiling.
- The thermal load on the engine structure is spatially non-uniform. Regions within close proximity experience different mechanisms of heat transfer. For example, on the flame deck, while heat is transferred by single phase forced convection in the region between the two intake valves, known as the intake valve bridge, occurrence of boiling is evidenced in the region between the two exhaust valves, the exhaust valve bridge.
- On account of the increased thermal load on the engine at maximum power load, the components experience significantly higher temperature and more heat transfer due to boiling, compared with the operation at maximum torque load.
- For a combination of low system pressure, low coolant flow rate and high bulk temperature of the coolant at inlet, occurrence of transition boiling is evidenced in the vicinity of the exhaust flange. Once transition boiling is encountered, for the operating condition with the lowest flow rate, any further decrease in system pressure resulted in a thermal run-away. The thermal run-away is characterized by a rapid increase in local metal temperature leading to an unstable operating condition. In such a scenario, the operator of the test rig intervened and increased the system pressure to prevent engine failure.

Båstedt et al. [2] presents and analyses the results from this thermal survey measurement campaign in detail.

## 5.3 Paper C: Numerical modelling of heat transfer in a four-cylinder petrol engine

In this study, the test conditions presented in Paper B are simulated and the performance of the BBM, i.e., the Blended Boiling Model, is evaluated using the measurement database obtained from the thermal survey measurement campaign. A complete engine 3D CFD-CHT simulation model of a four-cylinder Volvo passenger car petrol engine enabled the study of heat transfer in the engine. The commercial CFD solver, Star-CCM+ is used for the numerical analysis. The primary focus of this study is to analyse subcooled boiling flow in the coolant jacket. The engine structure and the coolant flow passages constituted the CFD-CHT model. The heat transfer coefficient and the reference temperatures, from dedicated in-cylinder combustion simulation and simulation of exhaust gases, are mapped onto the CFD-CHT model as convective boundary conditions on the gas side. The heat transfer coefficient and reference temperatures from dedicated CFD simulations of the heat transfer to the ambient air are specified as convective boundary conditions on the external surfaces of the engine. Also, convective boundary conditions are specified at the surfaces in contact with the lubricating oil. The CFD-CHT model resolves the heat

conduction in the engine structural components, the coolant flow and the associated heat transfer in the coolant jacket. The BBM, proposed in Paper A, is implemented in the CFD-CHT model. Virtual temperature probes are placed in the CFD-CHT simulation model at the locations of the thermocouples in the measurement campaign, enabling comparison of local metal temperatures.The key inferences from the numerical analysis are given below.

- The local metal temperatures estimated by the numerical simulations are within the accuracy of the measured temperatures in the exhaust valve bridge region.
- The simulation results are responsive to variation in system pressure and coolant flow rate, and are in good agreement with the measurements for the maximum torque load, both in the exhaust valve bridge and the exhaust flange regions.
- The simulation results deviate significantly from the measurements in the exhaust flange region for the maximum power load. This is on account of the extreme transition boiling experienced in this region. Estimating the heat flux in the transition boiling regime is outside the scope of the BBM.
- Although the BBM does not estimate the heat flux in the transition boiling regime accurately, the parameter indicating probability of bubble interaction, $\Pi$, indicates a value of 1 under such circumstances. Thereby, as described in Paper A, the parameter $\Pi$ could be used to estimate the extent of boiling and to know the limits of the beneficial partial boiling regime.

The numerical methodology and the results are presented in detail by Vasudevan and Bovo [3].

## 5.4 Paper D: Single phase and multiphase simulation frameworks for subcooled boiling flow

In this study, the BBM implemented in a single phase and the mixture multiphase CFD simulation frameworks are compared and evaluated with measurement results. Star-CCM+ is used for the numerical analysis. The single phase framework, on the one hand, does not account for the presence of the vapor phase and the thermal energy from the heated surface contributes only to increasing the internal energy of the liquid coolant, thereby, increasing its temperature. A suppression factor is incorporated that limits heat transfer from the wall in order to prevent the liquid temperature from exceeding the wall temperature. On the other hand, the mixture multiphase framework accounts for the phase change. In this framework, the transport equations of mass, momentum and energy are solved for a liquid-vapor mixture phase along with the transport equations for the volume fraction of the phases. Thereby, the mixture multiphase framework is computationally much less demanding compared with conventional two-fluid frameworks,

in which the transport equations are solved for the individual phases. The results from the single phase and the mixture multiphase frameworks are first compared and analysed with results from channel flow experiments by Steiner et al. [22]. Further, the two simulation frameworks are used to analyse heat transfer in the coolant jacket of a four-cylinder passenger car petrol engine. The important results and inferences from this study by Vasudevan et al. [4] are given below.

- In the channel flow simulations, the mixture multiphase framework is more accurate when the intensity of boiling is high due to low bulk flow velocity of the coolant. This is because of the increase in net vapor generated in the channel. However, with increase in bulk flow velocity, the results from the two frameworks are identical, since the vapor bubbles generated on the heated surface are convected by the flow and eventually condense in the liquid bulk. This results in insignificant net vapor generation.

- The accuracy of both the single phase and mixture multiphase frameworks are sensitive to the resolution of the computational grid. Excessive grid refinement, intending to resolve the viscous-sub layer, leads to inaccurate results.

- Four different operating conditions corresponding to the maximum power load, from the thermal survey measurements presented in Paper B, are chosen and simulated using the single phase and mixture multiphase frameworks. The local metal temperature estimated by the models are quite similar and are in reasonably good agreement with the measurements. Similar to results in Paper C, the BBM does not predict the heat transfer rate accurately in the transition boiling regime, but indicates a value of $\Pi \simeq 1$, in both the single phase and the mixture multiphase frameworks.

- Analysing the vapor bubble interactions in further detail, it is evident that the single phase framework estimates the parameter $\Pi$ conservatively. That is, the single phase framework indicates larger regions with higher probability of bubble interactions in the coolant jacket. In contrast, the multiphase framework estimates $\Pi$ more accurately.

From this study it is concluded that the single phase CFD framework is a powerful tool to analyse subcooled boiling flow in the coolant jacket of internal combustion engines, given the low demand for computational resources. However, if there is a need to analyse the effects of boiling in greater detail, with a goal of tapping the potential of nucleate boiling for improved cooling, the effect of phase change should be accounted for and for such analyses the mixture multiphase framework is suggested.

## 5.5 Paper E: Design and construction of a boiling rig

This technical report describes the design of the boiling rig located in Chalmers laboratory of Fluid and Thermal Science. The rig enables experimental investigation of subcooled boiling flow. Sensitivity to operating parameters, such as system pressure, coolant bulk temperature at inlet and coolant bulk velocity can be varied. Three different test specimens, made of copper, aluminium alloy and cast iron, are available for the experimental investigation. The primary test section is a square-sectioned channel with optical access to the boiling surface of the test specimen. Details regarding the other components of this closed circuit rig and the necessary instrumentation are elaborated in the technical report [5]. The report also presents a sample uncertainty calculation using data points from experiments of Lee and O'Niel [21]. While one of the data points is in the forced convection regime, the other is in the FDB regime. One dimensional heat transfer in the test specimen is assumed. Thermocouples are placed along the height of the specimen, which is along the direction of nominal heat flow, to estimate the wall temperature and the wall heat flux. Results from numerical simulations of heat transfer in the test specimen confirm that the heat conduction in the specimen is one dimensional.

# 6

# Concluding remarks

In the pursuit of minimizing the emission of greenhouse gases from road transport sector, especially from automobiles powered by internal combustion engines, minimizing the unintended heat loss to the coolant is realized as a viable option. In order to do so, precision cooling, i.e., selective removal of heat only from thermally critical regions, is preferred. Controlled local nucleate boiling is realized as a preferred alternative to the conventional heat transfer by forced convection in order to achieve enhanced precision cooling in internal combustion engines. Occurrence of nucleate boiling in conjunction with heat transfer by forced convection of a subcooled liquid increases the heat transfer rate exponentially and this type of boiling is known as subcooled boiling. The different boiling regimes within subcooled boiling flow and the complexities associated with different heat transfer mechanisms involved have been discussed in this thesis. The mechanisms of heat transfer are influenced by several parameters of the cooling systems, such as operating conditions, thermophysical properties of the liquid coolant and the heated solid, coolant composition, micro-structure of the heated surface, heated surface orientation and the like. These effects have been extensively discussed in the thesis based on data available in the literature. The thesis also presents a brief review of experimental and numerical studies in subcooled boiling flow, especially focused on heat transfer in the engine coolant jacket.

Nucleate boiling often occurs inadvertently in coolant jackets of engines with high specific power. While the conventional approach is to suppress nucleate boiling or to minimize its effects by increasing coolant flow rate, tapping the potential of nucleate boiling is more suitable for achieving enhanced precision cooling. One of the prerequisites for numerical analysis in the process of designing a boiling based engine cooling system is an efficient numerical wall boiling model. The model should predict the extent of boiling, in addition to estimating accurately the occurrence of boiling and the wall boiling heat flux. In line with this, a blended wall boiling model is proposed. The model blends two well established wall boiling models in the literature using a semi-mechanistic formulation of a blending parameter. The blending parameter estimates bubble interactions and thereby indicates the extent of boiling. This parameter is suggested to be used to limit boiling to the beneficial partial boiling regime and thereby avoid encountering critical heat flux with sufficient margin. Results from the proposed model are validated with experimental data available in the literature. The model is then implemented in a CFD-CHT simulation methodology to analyse subcooled boiling flow in the coolant jacket of a four-cylinder

passenger car petrol engine. A database of results from a dedicated thermal survey measurement campaign is used to evaluate the model performance. In the measurement campaign, the effect of varying the operating conditions of the cooling system are studied at two different engine operating loads. The results from the numerical simulations are in reasonably good agreement with the measurements, especially in the partial boiling and FDB regimes. The estimation of the extent of boiling using the blending parameter is also tested in conditions for which the occurrence of transition boiling is evidenced in the measurements. Based on the results, it is concluded that the blending parameter in the model indicates possible occurrence of the adverse boiling regimes under such conditions. Furthermore, the proposed boiling model is implemented in both a single phase and the mixture multiphase CFD frameworks. From a comparative analysis of the frameworks, it is inferred that the single phase framework is effective for the analysis of heat transfer in the engine coolant jacket, however, accounting for the vapor phase using the mixture multiphase framework is preferred when the focus is to explore the limits while tapping the potential of nucleate boiling.

The blended model has been evaluated based on measurement data available from one particular four-cylinder passenger car petrol engine. Evaluating the model for other engines and even other applications involving boiling based cooling systems would test the robustness of the model. This could include testing the model for applications involving heated solid materials other than aluminium alloy. Cast-iron is generally used in heavy duty engines and as mentioned previously, the thermal barrier effect in cast-iron makes numerical modelling of nucleate boiling more challenging. There is definitely scope for further work in this regard. Although the proposed boiling model indicates the limits of the partial boiling regime, it would be valuable to understand the proximity to critical heat flux once FDB is attained. Extending the model to estimate the critical heat flux and be able to specify a limit based on the critical heat flux will improve its versatility. Recently, Castiglione et al. [66] presented an optimal thermal management strategy, based on the 'Model Predictive Control' approach, targeting reduction of fuel consumption and $CO_2$ emission. In this approach, the coolant flow rate was regulated actively in a functional engine, based on live sensor data, in order to tap the potential of nucleate boiling. This was enabled by a zero-dimensional numerical boiling model which was programmed into the control unit in order to monitor the thermal state of the coolant. Using such an approach to test novel thermal management strategies with the boiling model proposed in this thesis is also a potential direction for future work.

The work also includes the design and construction of an experimental rig to investigate subcooled boiling flow. The rig offers possibility to test conditions similar to that in automotive engine coolant jacket. Future work also includes using the rig to test subcooled boiling flow of automotive coolant on specimens cut out from aluminium and cast-iron engines.

In summary this research effort provides a numerical methodology to estimate the occurrence, intensity and extent of nucleate boiling occurring in an ICE coolant jacket. This numerical methodology can potentially be an integral part of developing an enhanced precision cooling strategy targeting efficient vehicle thermal management.

# References


[1] S. Vasudevan, S. Etemad, L. Davidson, and G. M. Villar. Numerical model to estimate subcooled flow boiling heat flux and to indicate vapor bubble interaction. *International Journal of Heat and Mass Transfer* **170** (2021), 121038.

[2] P. Båstedt, S. Vasudevan, and M. Bovo. Subcooled Flow Boiling in High Power Density Internal Combustion Engines I: Thermal Survey Measurement Campaign. *SAE Int. J. Engines* **16**.1 (2023). https://doi.org/10.4271/03-16-01-0002..

[3] S. Vasudevan and M. Bovo. Subcooled Flow Boiling in High Power Density Internal Combustion Engines II: Numerical Modeling. *SAE Int. J. Engines* **16**.1 (2023). https://doi.org/10.4271/03-16-01-0003..

[4] S. Vasudevan, S. Etemad, L. Davidson, and M. Bovo. Comparative analysis of single and multiphase numerical frameworks for subcooled boiling flow in an internal combustion engine coolant jacket. *Applied Thermal Engineering* (revised manuscript submitted).

[5] S. Vasudevan and I. Jonsson. *Design and construction of a rig for investigation of subcooled boiling flow*. Tech. rep. Chalmers University of Technology, 2022.

[6] *Emissions of greenhouse gases from domestic transport by greenhouse gas and mode of transport. Year 1990 - 2020*. https://www.statistikdatabasen.scb.se/pxweb/en/ssd/START__MI__MI0107/MI0107InTranspN/table/tableViewLayout1/.

[7] R. Stone. *Introduction to internal combustion engines*. Macmillan International Higher Education, 2012.

[8] H. Kobayashi, K. Yoshimura, and T. Hirayama. *A study on dual circuit cooling for higher compression ratio*. Tech. rep. SAE Technical Paper, 1984.

[9] T. Hüttner and J. Hancock. Design and Evaluation of a Low Emission Spark Ignition Engine Cylinder Head. *SAE transactions* (1996), 730–741.

[10] R. P. Ernest. A Unique Cooling Approach Makes Aluminum Alloy Cylinder Heads Cost Effective. *SAE Transactions* (1977), 2882–2894.

[11] M. Clough. Precision cooling of a four valve per cylinder engine. *SAE Transactions* (1993), 1555–1566.

[12] I. Finlay, G. Gallacher, T. Biddulph, and R. Marshall. The application of precision cooling to the cylinder-head of a small, automotive, petrol engine. *SAE transactions* (1988), 399–410.

[13] K. Robinson, N. Campbell, J. Hawley, and D. Tilley. "A review of precision engine cooling". *International Congress & Exposition*. 1999-01-0578. 1998.

[14] M. Shoji. Studies of boiling chaos: a review. *International Journal of Heat and Mass Transfer* **47**.6-7 (2004), 1105–1128.

[15] H. Steiner, G. Brenn, F. Ramstorfer, and B. Breitschädel. Increased cooling power with nucleate boiling flow in automotive engine applications. *New trends and developments in automotive system engineering* (2011), 249–272.

[16] R. Judd and C. Lavdas. The nature of nucleation site interaction (1980).

[17] J. G. Collier and J. R. Thome. *Convective boiling and condensation*. Clarendon Press, 1994.

[18] Y. Y. Hsu. On the Size Range of Active Nucleation Cavities on a Heating Surface. *Journal of Heat Transfer* **84**.3 (Aug. 1962), 207–213. ISSN: 0022-1481. DOI: 10.1115/1.3684339.

[19] T. Sato and H. Matsumura. On the conditions of incipient subcooled-boiling with forced convection. *Bulletin of JSME* **7**.26 (1964), 392–398.

[20] N. A. Campbell. "The influence of nucleate boiling in engine cooling and temperature control". PhD thesis. University of Bath, 2001.

[21] H. Lee and A. O'Neill. Forced convection and nucleate boiling on a small flat heater in a rectangular duct: Experiments with two working fluids, a 50–50 ethylene glycol-water mixture, and water. *Proceedings of the Institution of Mechanical Engineers, Part D: Journal of Automobile Engineering* **223**.2 (2009), 203–219.

[22] H. Steiner, A. Kobor, and L. Gebhard. A wall heat transfer model for subcooled boiling flow. *International Journal of Heat and Mass Transfer* **48**.19-20 (2005), 4161–4173.

[23] E. Aktinol and V. K. Dhir. Numerical simulation of nucleate boiling phenomenon coupled with thermal response of the solid. *Microgravity Science and Technology* **24**.4 (2012), 255–265.

[24] U. Magrini and E. Nannei. On the influence of the thickness and thermal properties of heating walls on the heat transfer coefficients in nucleate pool boiling (1975).

[25] Z. Guo and M. S. El-Genk. Liquid microlayer evaporation during nucleate boiling on the surface of a flat composite wall. *International journal of heat and mass transfer* **37**.11 (1994), 1641–1655.

[26] L. Zou and B. G. Jones. Thermal interaction effect on nucleation site distribution in subcooled boiling. *International journal of heat and mass transfer* **55**.11-12 (2012), 2822–2828.

[27] L. Zou and B. G. Jones. Heating surface materials effect on subcooled flow boiling heat transfer of R134a. *International Journal of Heat and Mass Transfer* **58**.1-2 (2013), 168–174.

[28] C. French. Problems arising from the water cooling of engine components. *Proceedings of the Institution of Mechanical Engineers* **184**.1 (1969), 507–542.

[29] K. Robinson. "IC engine coolant heat transfer studies". PhD thesis. University of Bath, 2001.

[30] N. Campbell, J. Hawley, M. Leathard, R. Horrocks, and L. Wong. *Nucleate boiling investigations and the effects of surface roughness.* Tech. rep. SAE Technical Paper, 1999.

[31] B. Breitschädel. *Analyse des Wärmeübergangs beim unterkühlten Strömungssieden an metallischen Oberflächen.* na, 2008.

[32] H. Steiner, B. Breitschädel, G. Brenn, H. Petutschnig, and C. Samhaber. Nucleate boiling flow-experimental investigations and wall heat flux modelling for automotive engine applications. *Advd Computat. Methods Heat Transfer* **61** (2008), 169–178.

[33] M. J. Brusstar and H. Merte Jr. Effects of buoyancy on the critical heat flux in forced convection. *Journal of thermophysics and heat transfer* **8**.2 (1994), 322–328.

[34] J. S. Bower and J. F. Klausner. "Gravity independent subcooled flow boiling heat transfer regime". *Thermal Sciences 2004. Proceedings of the ASME-ZSIS International Thermal Science Seminar II.* Begel House Inc. 2004.

[35] C. Paz, M. Conde, J. Porteiro, and M. Concheiro. Experimental research of the effect of surface orientation on the subcooled flow nucleate boiling of water at low pressure (2016).

[36] S. G. Kandlikar and M. Bulut. An experimental investigation on flow boiling of ethylene-glycol/water mixtures. *J. Heat Transfer* **125**.2 (2003), 317–325.

[37] S. G. Kandlikar. Heat Transfer Characteristics in Partial Boiling, Fully Developed Boiling, and Significant Void Flow Regions of Subcooled Flow Boiling. *Journal of Heat Transfer* **120**.2 (May 1998), 395–401. ISSN: 0022-1481. DOI: 10.1115/1.2824263.

[38] S. Hua, R. Huang, Z. Li, and P. Zhou. Experimental study on the heat transfer characteristics of subcooled flow boiling with cast iron heating surface. *Applied Thermal Engineering* **77** (2015), 180–191.

[39] H. Z. Abou-Ziyan. Forced convection and subcooled flow boiling heat transfer in asymmetrically heated ducts of T-section. *Energy conversion and management* **45**.7-8 (2004), 1043–1065.

[40] A. Torregrosa, A. Broatch, P. Olmeda, and O. Cornejo. Experiments on subcooled flow boiling in IC engine-like conditions at low flow velocities. *Experimental thermal and fluid science* **52** (2014), 347–354.

[41] N. Koumoutsos, R. Moissis, and A. Spyridonos. A study of bubble departure in forced-convection boiling (1968).

[42] V. Sernas and F. Hooper. The initial vapor bubble growth on a heated wall during nucleate boiling. *International Journal of Heat and Mass Transfer* **12**.12 (1969), 1627–1639.

[43] J. Klausner, R. Mei, D. Bernhard, and L. Zeng. Vapor bubble departure in forced convection boiling. *International journal of heat and mass transfer* **36**.3 (1993), 651–662.

[44] R. Benjamin and A. Balakrishnan. Nucleation site density in pool boiling of saturated pure liquids: effect of surface microroughness and surface and liquid physical properties. *Experimental Thermal and Fluid Science* **15**.1 (1997), 32–42.

[45] N. Basu, G. R. Warrier, and V. K. Dhir. Onset of nucleate boiling and active nucleation site density during subcooled flow boiling. *J. Heat Transfer* **124**.4 (2002), 717–728.

[46] C. Wang and V. Dhir. On the gas entrapment and nucleation site density during pool boiling of saturated water. *Journal of Heat Transfer* **115**.3 (Aug. 1993), 670–679. ISSN: 0022-1481. DOI: 10.1115/1.2910738.

[47] A. Calka and R. L. Judd. Some aspects of the interaction among nucleation sites during saturated nucleate boiling. *International journal of heat and mass transfer* **28**.12 (1985), 2331–2342.

[48] R. Judd and A. Chopra. Interaction of the nucleation processes occurring at adjacent nucleation sites (1993).

[49] S. Siedel, S. Cioulachtjian, and J. Bonjour. Experimental analysis of bubble growth, departure and interactions during pool boiling on artificial nucleation sites. *Experimental Thermal and Fluid Science* **32**.8 (2008), 1504–1511.

[50] T. Bo. *CFD homogeneous mixing flow modelling to simulate subcooled nucleate boiling flow*. Tech. rep. SAE Technical Paper, 2004.

[51] W. M. Rohsenow. *A method of correlating heat transfer data for surface boiling of liquids*. Tech. rep. Cambridge, Mass.: MIT Division of Industrial Cooporation,[1951], 1951.

[52] B. Petukhov and V. Popov. Theoretical Calculation of Heat Exchange in Turbulent Flow of Liquids in Tubes of an Incompressible Fluid with Variable Physical Properties'. *High Temp* **1**.1 (1963), 69–83.

[53] W. Bowring. "Physical model of bubble detachment and void volume in subcooled boiling". *OECD Halden Reactor Project Report No. HPR-10*. 1962.

[54] S. Mohammed and M. Shah. A general correlation for heat transfer during subcooled boiling in pipes and annuli. (1977).

[55] V. Prodanovic, D. Fraser, and M. Salcudean. On the transition from partial to fully developed subcooled flow boiling. *International journal of heat and mass transfer* **45**.24 (2002), 4727–4738.

[56] J. C. Chen. Correlation for boiling heat transfer to saturated fluids in convective flow. *Industrial & engineering chemistry process design and development* **5**.3 (1966), 322–329.

[57] F. Dittus and L. Boelter. University of California publications on engineering. *University of California publications in Engineering* **2** (1930), 371.

[58] H. Forster and N. Zuber. Dynamics of vapor bubbles and boiling heat transfer. *AIChE Journal* **1**.4 (1955), 531–535.

[59] N. Kurul and M. Z. Podowski. "Multidimensional effects in forced convection subcooled boiling". *International Heat Transfer Conference Digital Library*. Begel House Inc. 1990.

[60] H. Punekar and S. Das. *Numerical simulation of subcooled nucleate boiling in cooling jacket of IC engine*. Tech. rep. SAE Technical Paper, 2013.

[61] S. Das and H. Punekar. On Development of a Semimechanistic Wall Boiling Model. *Journal of Heat Transfer* **138**.6 (2016).

[62] H. Petutschnig, P. Klinner, A. Kobor, and E. Schutting. Numerical computation of the temperature field in the cylinder heads of modern high-speed diesel engines. *MTZ worldwide* **63**.12 (2002), 6–9.

[63] V. Prulj and M. Shala. Multi-phase mixture modelling of nucleate boiling applied to engine coolant flows. *Computational Methods in Multiphase Flow V* **63** (2009), 135–146.

[64] S. Hua, R. Huang, and P. Zhou. Numerical investigation of two-phase flow characteristics of subcooled boiling in IC engine cooling passages using a new 3D two-fluid model. *Applied Thermal Engineering* **90** (2015), 648–663.

[65] T. Mazzocco, W. Ambrosini, R. Kommajosyula, and E. Baglietto. A reassessed model for mechanistic prediction of bubble departure and lift off diameters. *International Journal of Heat and Mass Transfer* **117** (2018), 119–124.

[66] T. Castiglione, F. Rovense, A. Algieri, and S. Bova. *Powertrain thermal management for CO2 reduction*. Tech. rep. SAE Technical Paper, 2018.